NOTICE: When government or other drawings, specifications or other data are used for any purpose other than in connection with a definitely related government procurement operation, the U. S. Government thereby incurs no responsibility, nor any obligation whatsoever; and the fact that the Government may have formulated, furnished, or in any way supplied the said drawings, specifications, or other data is not to be regarded by implication or otherwise as in any manner licensing the holder or any other person or corporation, or conveying any rights or permission to manufacture, use or sell any patented invention that may in any way be related thereto.

RADC-TR-60-236

OCTOBER 1960

METAL-TO-CERAMIC SEAL TECHNOLOGY STUDY

FINAL TECHNICAL REPORT

Covering the Period

22 June 1959 to 22 September 1960

ELECTRONIC TUBE DIVISION
SPERRY GYROSCOPE COMPANY
DIVISION OF SPERRY RAND CORPORATION
GREAT NECK, NEW YORK

SPERRY REPORT NO. NA-8240-8216

CONTRACT NO. AF 30(602)2047

PREPARED FOR

ROME AIR DEVELOPMENT CENTER
AIR RESEARCH AND DEVELOPMENT COMMAND
UNITED STATES AIR FORCE
GRIFFISS AIR FORCE BASE
NEW YORK

RADC-TR-60-236

COPY NO. 41

OCTOBER 1960

METAL-TO-CERAMIC SEAL TECHNOLOGY STUDY

FINAL TECHNICAL REPORT

Covering the Period

22 June 1959 to 22 September 1960

ELECTRONIC TUBE DIVISION

SPERRY GYROSCOPE COMPANY

DIVISION OF SPERRY RAND CORPORATION

GREAT NECK, NEW YORK

SPERRY REPORT NO. NA-8240-8216

CONTRACT NO. AF 30(602)2047

PROJECT NO. 4506 TASK NO. 45152

PREPARED BY

ENGINEERING DEPARTMENT

S. S. Cole, Jr.

H. W. Lorisch

J. E. Inge

K. H. Styhr, Jr.

PUBLICATIONS DEPARTMENT

E. Cheetham

PREPARED FOR

ROME AIR DEVELOPMENT CENTER

AIR RESEARCH AND DEVELOPMENT COMMAND

UNITED STATES AIR FORCE

GRIFFISS AIR FORCE BASE

NEW YORK

TABLE OF CONTENTS

TABLE OF CONTENTS (Cont)

TABLE OF CONTENTS (Cont)

APPENDIX - TABLES

TABLE OF CONTENTS (Cont)

TABLE OF CONTENTS (Cont.)

LIST OF ILLUSTRATIONS

LIST OF ILLUSTRATIONS (Cont)

FOREWORD

This study was conducted by the Techniques Section of the Electronic Tube Division, Sperry Gyroscope Company Division of Sperry Rand Corporation, Great Neck, New York. The Sperry Materials Laboratory also participated in the program; this group was responsible for the stress analysis portion of the study and for other metallurgical and measurement aspects. Sincere appreciation is expressed to Lt. Charles Martin of RADC, the Contract Officer; Mr. James McLinden of Sperry, Techniques Section Head; Mr. Frank Vanderveer of the Sperry Materials Laboratory; and to the many other individuals whose contributions made the work possible.

ABSTRACT

To achieve ceramic-to-metal seals demonstrating strengths as high as the ceramic member itself required a thorough testing program for their measurement and evaluation. A study was also conducted on the analytical and experimental nature of seal stresses.

A literature survey on ceramic-to-metal sealing techniques, adherence theory, and allied systems disclosed limited published work and no procedures for achieving ultra-high-strength seals or seals to pure high alumina. Reported work on adherence mechanisms is limited to chemical reaction and molybdenum oxide reaction theories.

Two additional theories were formulated for this study--one proposing the migration of the glass in the ceramic into the metallizing mixture, and the other recognizing the need for promoting metallizing sintering. These theories, together with thermodynamic and equilibrium calculations, allowed 200 metallizing compositions to be formulated.

Three sintering temperatures were chosen, depending on composition, for each of the 200 metallizing mixtures. Each mixture was applied to specimens of 94-, 96-, and 99.6-percent alumina. Testing involved a screening technique whereby the most promising compositions were carried through to increasingly refined test techniques (scratch and peel, circumferential seal, and finally tensile tests). Approximately 3200 specimens were prepared and tested.

The tensile test specimen was redesigned to eliminate shoulder breaks when evaluating ultra-high-strength seals. A photoelastic study was made to learn more about stress distribution in this specimen.

Extremely strong seals were developed for all the ceramic bodies considered. A wide variety of sealing compositions was disclosed which produced seals stronger than those previously reported. Careful analysis of the data indicated that the Glass Migration Theory should receive careful consideration and that simple chemical reactions were not enough to explain seal adherence.

A study was made of the origin and nature of seal stresses resulting from the dissimilar physical properties of metals and ceramics. A method to calculate stresses in ceramic-to-metal seals is theorized. Measurements of the properties of the metal and of residual stresses in seals were made, showing excellent agreement with calculated stresses.

SECTION A

INTRODUCTION

1. PURPOSE OF PROGRAM

This final report, discussing a study of metal-to-ceramic seal technology, has been prepared for the U.S. Air Force Air Research and Development Command by the Sperry Gyroscope Company Division of Sperry Rand Corporation, Great Neck, New York. The work described herein was performed under Contract No. AF30(602)2047 during the period 22 June 1959 to 22 September 1960.

The objective of this study was to advance ceramic-to-metal seal technology to the point where stronger seals--seals with bond strengths approaching tensile strengths of 25,000 psi, the strength of the ceramic member--could be developed and produced. It was anticipated that through theoretical and experimental investigations, seals would be developed which not only were stronger as far as bond strength was concerned, but also would be more satisfactory in meeting the demands for increased electrical, mechanical, and thermal requirements which are being imposed by present and future high-performance electronic-tube applications.

Two major directions were explored to fulfill the goal of the program. The first was a compilation of possible metallizing mixtures through theoretical considerations such as high-temperature phase equilibria, thermodynamics, and equilibria calculations, with subsequent experimental fabrication and testing of 200 of the most promising mixtures. The second direction was an analytic and experimental investigation

of the stresses developed at the ceramic-metal interface due to differences in the coefficients of thermal expansion of the metals and the ceramics. High-temperature properties of several metals and ceramics were measured, and stresses in the ceramic-metal interface were predicted on the basis of these data. A method of calculating stresses knowing the physical properties of the materials involved was determined. These calculated stresses were then compared with stresses actually measured in fabricated ceramic-to-metal seal assemblies.

Two technical papers resulted from this contract and a third is anticipated. These were "Theory of Adherence in Ceramic-to-Metal Seals" by S.S. Cole, Jr., and H.W. Larisch, presented at the Fifth Tube Techniques Conference; "The Glass Migration Mechanism of Ceramic-to-Metal Seal Adherence" by S.S. Cole, Jr., and G. Sommer, presented at the Electronic Division of the American Ceramic Society; and "The Calculation of Stress in Ceramic-to-Metal Seals" by S.S. Cole, Jr., and S. Inge, which is proposed for presentation at the Annual Meeting of the American Ceramic Society.

2. PHASES OF THE PROGRAM

The goal of this program was achieved through six major phases of study, the first five of which were intimately interdependent. These were as follows:

a. Phase I - Literature Survey and Analysis - A general survey was made of all literature related to ceramic-to-metal seal technology. This survey included a study of ceramic-metal reactions which were not necessarily related to common seal technology, but were useful in gaining more fundamental knowledge concerning bond mechanisms.

b. Phase II - Metallizing Investigation - A comprehensive investigation of metallizing materials and their fabrication, application, and processing was conducted. Phase equilibria, thermodynamics, and previous work in this field were considered. Two hundred experimental metallizing compositions were prepared and tested by a series of successfully refined tests. Efforts were made to relate data to the nature of the bond mechanism or mechanisms between various metallizing materials and ceramics.

c. Phase III - Brazing Investigation - An investigation of the effect of solders, their composition, thickness, time in the liquid state, the effect of weights, and the role of the metal members on brazing was planned. However, this phase was not necessary to fulfill the purpose of the program. Conventional brazing techniques were used capable of producing the desired strengths provided a metallizing mixture was properly sintered onto any particular ceramic in question.

d. Phase IV - Testing Investigation - A broad and definitive testing program was undertaken to evaluate testing techniques and variables. Testing methods included the torque peel, drum peel, tensile, and compression tests, and also the leak checking of compression-test assemblies. A comparison of testing methods was conducted on a standardized metallizing mixture, which was applied, sintered, and brazed under standardized conditions. The results of this comparison were statistically analyzed.

e. Phase V - Temperature Investigation - This phase was a study of the effect of temperature cycling on seal strength and seal vacuum tightness from sub-zero to elevated temperatures.

f. Phase VI - Stress Investigation - A study of the stresses involved in simple ceramic-to-metal seal structures due to differences between the thermal expansion rates of metals and of ceramics was conducted. To gain basic knowledge in these areas, comparisons were made between calculated and measured stresses in ceramic-to-metal seal assemblies.

SECTION B

DISCUSSION

3. PHASE I - LITERATURE SURVEY AND ANALYSIS

a. Introduction

Phase I consisted of a review of published literature concerning ceramic-to-metal seals, with particular emphasis direct l toward the refractory-metal process because of its wide use in the electronic-tube industry. To metallize metal-ceramic seals by the refractory-metal process, a thin coating of finely ground metal particles is placed on the ceramic surface and heated to temperatures in the range of 1200°C to 1300°C. During the heating process, the metal particles sinter and adhere to the ceramic and to each other. The result is a hard, rough coating to which other metals can be bonded. The metallizing is electrically conductive; but because of its extreme thinness. it does not lend itself to the common metal-working processes such as machining or drilling.

A wide variety of metals were found satisfactory for the metallizing process. Historically, the first refractory-metal seals were composed of molybdenum or tungsten metal and iron.[2,3*] Various additions were made to the molybdenum or tungsten, including manganese, titanium, nickel, iron oxide, manganese oxide, and glasses. In addition to being carried out in a vacuum, the sintering process was conducted in atmospheres of hydrogen, argon, dissociated ammonia, producer gas, and natural gas.

- - - - - - -

*The references cited are located in the Bibliography following the text.

The investigation of adherence mechanisms revealed a state of considerable complexity and one not easily satisfied by any single theory. This condition was further complicated by the fact that within the refractory-metal or Telefunken sealing group there are several basic types of metallizing mixtures which are placed on various high-alumina ceramics (ranging from 85-percent to almost 100-percent alumina). It is likely that different adherence mechanisms are operative as the metallizing types and alumina content of a body are changed.

b. Alumina Reaction Theory of Adherence

The earliest references of adhering molybdenum and tungsten seals to ceramics are by H. Pulfrich[4-10] and H. Vatter[11-16]. Working basically with steatite rather than high-alumina bodies, Pulfrich was nevertheless aware of the role of chemical reactions and liquid phases. He recognized the need to heat the metallizing to temperatures which approach softening or eutectic points in the ceramic. Pulfrich stated that the furnace atmosphere should contain sufficient hydrogen to maintain most of the molybdenum as a metal, but also sufficient oxygen (about 0.25 percent) to form a trace of molybdenum oxide. This oxide was said to melt and flow to the ceramic surface and there promote bonding. The possibility that adherence may be due to the glassy phase of the ceramic was also recognized.

In 1953, Pincus, after considering some basic chemical reactions and after several microscopic observations, drew some basic conclusions[17]. He postulated that manganese in a wet hydrogen atmosphere will oxidize to manganous oxide, a reaction completed at 1000°C. As the temperature increases,

a solid-state reaction begins to form the compound manganese aluminate, $MnO \cdot Al_2O_3$, also called manganese spinel. A further increase in temperature produces a molten or slag condition of this compound at the ceramic-metal interface. At 1400°C, an appreciable sintering of molybdenum particles to each other has taken place, and the spinel has begun to lock this hardened layer to the ceramic. Increasing the temperature further causes the mass of manganese spinel to begin to crystallize, thereby forming galaxite, a second crystalline form of spinel. Finally, precipitation of corundum (Al_2O_3) crystals will occur. This precipitation, Pincus advocates, heralds the general weakening of the seal.

The Alumina Reaction Theory predicts that seals made to a 100-percent alumina body should be as strong, or stronger, than those made to a 90-percent alumina body. Experimentally it has been universally observed that as the alumina content increases seals become more difficult to make.

In a later paper on adherence mechanisms, Pincus postulated that bonds between pure molybdenum and high-alumina ceramics, though weak, were chemical in nature and depended upon a reaction between molybdenum oxide and aluminum oxide[18]. A number of reasons exist which cause certain doubt. Molybdenum oxide, either MoO_2 or MoO_3, has never been reported as occurring after firing molybdenum metal in a hydrogen atmosphere. An argument has been put forth that hydrogen atmospheres heavily laden with water vapor will supply the necessary oxygen to allow the reaction

$$Mo + 2H_2O \longrightarrow 2H_2 + MoO_2$$

to take place. Although this reaction is thermodynamically predictable at rather low temperatures[19-23], repeated attempts

to achieve it at Sperry and at other organizations have failed. Even if the oxide is formed, for example, by heating in air or by prolonged low-temperature heating in wet hydrogen, it is so volatile that it immediately vaporizes at temperatures higher than 600°C to 700°C.

An immediate question concerns the purpose of water vapor in hydrogen gas. To form spinel, it is necessary to satisfy the reaction

$$Mn + H_2O \longrightarrow MnO + H_2$$

A second important function is in the promotion of sintering, as water vapors are known to aid sintering to a very marked degree.

It is questionable whether the molybdenum-iron system will behave the same. To date, no work has been reported, probably because of the comparatively small use of this mixture. A suspicion that there is considerable complicity in this system is warranted because the reaction

$$Fe + H_2O \longrightarrow FeO + H_2$$

can be expected to be highly temperature and dew-point sensitive, as predicted by thermodynamic calculations.

Denton and Rawson investigated two refractory-metal techniques, namely the molybdenum-manganese and the molybdic trioxide techniques[24]. The importance of the minor constituents of the ceramic in the sealing mechanism is pointed out in their paper. They conclude that in the molybdenum-manganese technique, acidic oxides, such as SiO_2, are likely to have an important effect on the metallizing behavior on the ceramic. In the molybdic trioxide technique, however, basic oxides,

such as MgO and CaO, may be more important. Denton and Rawson also conclude that the texture of the ceramic is of importance in controlling the interaction between the ceramic and the metallizing layer, fine grain ceramics being, in general, easier to metallize. The Alumina Reaction Theory is supported by these researchers.

c. Glass Phase Migration Theory of Adherence

In contrast to the type of mixture in which 15 to 30 percent of the mix is manganese, iron, or some other metal, a second basic metallizing type can be considered. This is the group in which the metallizing mixture is largely molybdenum and a small addition of an active material, usually titanium. Working with a mix of 94-percent molybdenum and 6-percent titanium, Cole and Hynes investigated the effect of ceramic composition on seal strength[25]. This work suggested dependence of seal strength on both glass content and glass composition within the high-alumina body. No attempt was made to theorize a sealing mechanism, although subsequent studies pointed to a very probable mechanism in this system. Titanium, like manganese, will readily form an oxide in a wet hydrogen atmosphere according to the reaction

$$Ti + 2H_2O \longrightarrow TiO_2 + 2H_2$$

It is very probable that the titanium dioxide enters the glassy phase of the ceramic and causes a reduction in viscosity. This, in turn, enables the glass to flow slightly and enter the interstices of the molybdenum coating. Microscopic examinations supported this theory; in addition, the decrease in seal strength with increasing alumina content is predictable.

d. Other Factors Affecting Adherence

Although adherence of the molybdenum to the ceramic is the most elusive aspect of ceramic seals, there are other facts to consider. The plating of the molybdenum coating adheres to the metallized coating because of mechanical means. This plating is not well bonded and may be easily peeled off if it is allowed to become too thick. If, however, the plated coating is fired, a solid-state sintering reaction occurs between the molybdenum particles adhering to the ceramic and the plated metal. The rough and somewhat porous molybdenum boundary layer, into which the plated metal has diffused, can be seen under a microscope. It was observed that this diffusion is substantially increased by firing the coating.

Whether or not the plate is fired prior to brazing is a disputable question, because it undergoes a heating operation during brazing. What actually happens during brazing depends mainly on what solders and plates have been chosen. If copper plate and copper solder are used, both will melt and enter the porous molybdenum coating heavily. If a higher melting plate is used (for example, copper-plated metal member and silver-copper eutectic solder, or nickel-plated metal member and copper solder), the occurrences in brazing are complicated. Phase diagrams found in the Metals Handbook[26] are helpful in this respect. In general, the solder will react with the plate and the final alloy can be roughly estimated by use of the phase diagrams. The degree of reaction will be determined by the plating thickness and by the amount of time the solder is allowed to remain liquid. Usually a microscopic examination of the seal will not show any trace of the plate. However, this is not always true; occasionally the resulting graded alloy will be seen, or the plate can be observed to be

nearly unaffected by the solder. Concern about the intricacies of the brazing operation becomes a secondary problem because seals have been found to fail repeatedly at the ceramic-to-metal interface.

e. Related Systems and Porcelain-Enamel Reactions

Some qualitative information from related systems, such as the fabrication of cermets, and also from porcelain-enamel reactions aided in the understanding of seal mechanisms. The reactions which take place during the formation of cermet bodies occur, in the majority of cases, between ceramic-type materials such as titanium or silicon carbide, and metals such as iron, nickel, and chromium and/or alloys such as Haynes Alloy No. 1, Haynes Alloy No. 25, and Nichrome. These reactions involve the dispersing of the ceramic constituent in the form of grains within a continuous metallic phase. The dispersing takes place during a liquid- or solid-state sintering operations such as (1) hot pressing (simultaneous heating and pressing in an induction furnace in the presence of a protective atmosphere), (2) cold pressing and subsequent sintering in a protective atmosphere furnace, or (3) vacuum infiltration (diffusion of metal or alloy into a ceramic-type porous skeleton material in a vacuum furnace).

Porcelain-enamel reactions occurring in the fusing of fritted glasses to hot-rolled enameling iron involve the interaction of oxides, carbonates, nitrates, and fluorides (after their smelting, in which case the less stable carbonates and nitrates are converted to stable oxides) with iron and its various oxides in the presence of heat. The adherence phenomena present after these reactions have been completed are complex and subject to continual review and debate. Neither of the two forementioned subjects seem to involve reactions of alumina and metal to any extent.

4. PHASE II - METALLIZING INVESTIGATION

a. Investigation Design

The metallizing investigation, one of the major efforts in this study, was developed around five basic sealing mechanisms. These are:

- The Alumina Reaction Theory, which depends on a chemical reaction of the metallizing composition and the ceramic.
- The Molybdenum Oxide Theory, which depends on the reaction of molybdenum oxide with ceramic.
- The Glass Migration Theory, which depends on glass migration from the ceramic into the metallizing coating.
- The Molybdenum Sintering Mechanism, which recognizes the need for adequate molybdenum sintering.
- The Glass Additive Mechanism, which suggests that seals can be accomplished by adding glass to the metallizing composition.

In addition, a category of compositions which does not appear to conform to any theory, but which has been reported to be of high seal strength was investigated.

The above categories, used with thermodynamic and equilibrium-diagram data where possible, allowed the formulation of the 200 metallizing compositions listed in the various tables in the Appendix. These compositions were determined in the following manner.

(1) Alumina Reaction Theory

The Alumina Reaction Theory, as proposed by A. Pincus, predicts a compound formation between the alumina and one of the metals used in the metallizing mixtures. By measuring the free energies and heats of formation in related chemical reactions, it is possible to predict whether other reactions can be expected to occur. As an example of such a thermodynamic prediction, water has a free energy of formation of -52,360 calories per mole* at a temperature of 500°K. This can be written as

$$H_2 + \tfrac{1}{2}O_2 \longrightarrow H_2O; \Delta F = -52{,}360 \text{ cal}$$

At the same temperature, the reduction of titanium dioxide can be written as

$$TiO_2 \longleftarrow Ti + O_2; \Delta F = +203{,}450 \text{ cal}$$

To predict the reaction of titanium metal with water vapor or hydrogen, such as is present in sintering furnaces, the above reactions are added:

$$2H_2 + O_2 \longrightarrow 2H_2O; \quad \Delta F = -104{,}720 \text{ cal}$$
$$TiO_2 \longleftarrow Ti + O_2; \quad \Delta F = +203{,}450 \text{ cal}$$
$$2H_2 + TiO_2 \longleftarrow Ti + 2H_2O; \Delta F = +98{,}730 \text{ cal}$$

Because this reaction has a positive free energy, it will proceed to the left, forming TiO_2 at 500°K, providing there is no very large excess of hydrogen present. However, in a wet hydrogen atmosphere, a large excess of hydrogen is present. If the water content becomes low enough, the reaction will tend to drive to the right despite the large positive ΔF. This possibility

- - - - - - -

*The minus sign indicates the tendency for the reaction to proceed to the right; a positive ΔF indicates a tendency to proceed to the left.

may be predicted by a consideration of the partial pressures of the two gases, hydrogen and water vapor, which are present. These factors are related by the following formula:

$$\Delta F = -RT \ln \frac{PH_2O}{PH_2} \text{ (at equilibrium)}$$

which is rewritten as

$$\ln \frac{PH_2O}{PH_2} = -\frac{\Delta F}{RT}$$

where

PH_2O = partial pressure water

PH_2 = partial pressure hydrogen

F = free energy of reaction

R = molar gas constant

T = absolute temperature

If $\ln(PH_2O/PH_2)$ is numerically greater than $-\Delta F/RT$, the equation will not be satisfied and the titanium will tend to oxidize. However, if $\ln(PH_2O/PH_2)$ is less than $-\Delta F/RT$, reduction can be predicted. At a dew point of 0°C,

$$\ln \frac{PH_2O}{PH_2} = -3.4$$

and at 500°K,

$$-\frac{\Delta F}{RT} = -98$$

Oxidation can be expected because $\ln(PH_2O/PH_2)$ is numerically greater than $-\Delta F/RT$. Previously, this has been proven valid by experimental means. It can further be shown that a dew point of about -10^4°C is required at 500°K to cause TiO_2 to

reduce. As in all cases, it must be pointed out that thermodynamic predictions do not consider reaction rate or any of several other factors which may slow or stop a reaction from proceeding; these are, nevertheless, very accurate predictions.

Having predicted whether an oxide or a metal will be present, it is possible to predict from phase diagrams the reactivity of aluminum oxide with other oxides. The diagrams also give a good indication of the temperatures at which the reactions can be expected to occur. Table 1* lists the metals whose oxides will react with aluminum oxide, their tendency to oxidize, the melting point of the metal and its oxide, and the lowest melting eutectic between Al_2O_3 and the metallic oxide. From this table, compositions have been formulated which should behave according to the alumina reaction mechanism. These are shown in table 2.

(2) Molybdenum Oxide Theory

The second category (suggested by Pincus) is based on the chemical reaction between the primary material and the ceramic. This would involve, for example, the formation of a small amount of molybdenum oxide, which would then react in the same fashion with the ceramic. Table 3 lists the compositions containing additions of MoO_3 to apply this theory of adherence.

(3) Glass Migration Theory

The Glass Migration Theory, which recognizes the importance of the glassy phase in the ceramic, was developed from the work conducted by Cole and Hynes[25]. It is proposed

- - - - - - -

*Tables are grouped in numerical order at the rear of the report.

that certain metals, such as titanium, after having oxidized in a wet hydrogen atmosphere enter the glassy phase of the ceramic and lower the viscosity of that glass. The glass is then free to flow out slightly and lock the ceramic to the somewhat porous molybdenum coating which remains.

An entirely different direction is used in the approach to the Glass Migration Theory. Over the period of a great many years, the glass, enamel, and glaze manufacturers have been able to determine the materials which are known to lower the viscosity of glasses; a substantial list of materials has evolved which is suspected to affect greatly glass viscosity. These are shown in table 4 along with their principal sources. From this table, compositions were made which should behave according to the theory (see table 5).

(4) Molybdenum Sintering Mechanism

The sintering mechanism recognizes the need for accomplishing thorough sintering of the molybdenum particles and cells. For sintering to occur, the sintering particles must be in intimate contact with each other so that bonding can take place at the point of contact. Theoretically, anything which would increase this contact area would enhance subsequent sintering by supplying more bonding points. Any increase in temperature not above the melting point will enhance the sintering rate because of increased diffusion rate and plastic deformation.

From the standpoints of mutual solubility, crystal structure, and atomic size, the following elements were predicted for addition: titanium, vanadium, chromium, iron, cobalt, nickel, zirconium, niobium, and tantalum. Of these, only iron,

nickel, and cobalt will not oxidize in a wet hydrogen atmosphere according to thermodynamic calculations. Compositions formulated on the basis of these considerations are shown in table 6.

(5) Glass Additive Mechanism

This mechanism postulates that glassy or glass-forming materials can be added to a metallizing mixture composed basically of a refractory metal such as molybdenum. The glass thus added is then able to fuse to both the ceramic and the metal particles.

A series of compositions based on the Glass Additive Mechanism were made (table 7). They were largely determined by an extensive literature search and a study of previous work by other researchers in this field. Certain problems arise in a study of this mechanism. The glass must have a high softening point, must be capable of wetting both the high alumina and the molybdenum grain, and must have fair mechanical strength. However, the glass must not be reduced in a wet hydrogen furnace.

(6) Other Mechanisms

In addition to the above, the literature search yielded a series of compositions which were considered worthy of trial at various temperatures and on the various high-alumina bodies. These compositions are shown in table 8.

b. Evaluation of Metallizing Compositions

(1) Materials and Methods

Based on the above information, the ceramics listed on the following page were chosen to be metallized and evaluated. These are typical high-alumina ceramics which are of interest to the electronic-tube industry.

- AD-94 - A dense 94-percent alumina body manufactured by the Coors Porcelain Co.
- AD-96 - A dense 96-percent alumina body manufactured by the Coors Porcelain Co.
- AL-23 - A dense 99.6-percent alumina body supplied by Materials For Electronics, Inc.

The following milling procedures were used:

- Inside dimensions of the steel mills, selected because of their capability for more efficient grinding than porcelain, are 5.5 x 6 inches.
- 0.5-inch-diameter steel balls were placed 2 inches deep in the bottom of the mill. About six one-inch steel balls were also added to each mill.
- Materials shown in tables 2 through 8 were weighed and placed in the mill.
- A binder of 60 ml acetone, 60 ml amyl acetate, and 25 ml 8-percent nitrocellulose lacquer was added.
- If, after 2 hours of milling, viscosity was not less than 50 cps, binder additions were made in quantities of 70 ml until the viscosity was less than 50 cps.
- Milling was conducted for 24 hours at a mill speed of 60 rpm.
- Mills were emptied and cleaned with acetone prior to recharging.
- Resulting mixtures were stored in glass jars with polyethylene-lined caps.

The compositions were then sintered to various ceramics at various temperatures, and tested by a successive series of tests designed to be more exacting as the less promising compositions were eliminated.

(2) Adherence Test

Three different metallizing compositions were painted on 1.5-inch discs of each of the three ceramics studied (see figure 1). These were then sintered in molybdenum boats, each holding 27 discs. The furnace atmosphere was wet dissociated ammonia, the dewpoint of which was held between +80°F and +85°F by passing the furnace gasses through a controlled-temperature water tank. Figure 2 illustrates the furnace-temperature profile and the sintering cycle of the metallized ceramics for the 1300°C sintering temperature. The same sintering cycle in a furnace-temperature profile similar to that shown in figure 2 was used in the firings at 1250°C, 1350°C, 1400°C, and 1500°C. Because of a furnace limitation, a different furnace was required for the 1600°C and 1700°C sinterings; the same atmosphere, dewpoint, and 30-minute time period in the hot zone of the furnace were used.

After sintering, the coatings were adherence tested using a scalpel and 30-power binocular microscope. A system of rough grading the coatings was devised as follows:

- Poor — no adherence, coatings curl, no effort expended in removal , cracks or holes visible.
- Fair — moderate adherence, moderate coating hardness and cohesion.
- Good — metallizing coating absolutely not removable, ceramic removed, hard dense metal films.

Results of the adherence tests conducted on all discs sintered at all proposed temperatures are shown in tables 2 through 8. The adherence testing program was originally

designed to eliminate only those experimental metallizing mixtures which exhibited grossly poor adherence, at all sintering temperatures, to all three ceramic bodies considered in this program. It soon became apparent that few metallizing mixtures could be eliminated by this technique. No mixtures yielded poor ratings to all ceramics at all temperatures, and few were found that could not be rated at least fair or fair-to-good on some ceramics at some sintering temperatures. Peel tests were next performed on all stripes of experimental metallizing mixtures resulting from the adherence test program. Because both tests were conducted on all combinations of mix, body, and sintering temperature, results of both tests are discussed concurrently in the following paragraphs.

(3) Torque Peel Test

The torque peel test was chosen as a quick, inexpensive test of ceramic-to-metal seal strength from the results of Phase IV, Testing Investigation. After completing the adherence test, each stripe of experimental metallizing on all discs of each of the three bodies was plated with 0.0005-inch hard nickel. A 1.25- x 0.375- x 0.010-inch Kovar strip was then brazed to each stripe using a 0.002-inch shim of OFHC copper. These Kovar strips were then peeled from the ceramic by the torque wrench and torque peel fixture illustrated in figure 3.

Results of the torque peel tests are also included in tables 2 through 8. The massive amount of data contained in these tables was difficult to analyze and was therefore handled in the following manner. All metallizing compositions were separated into groups according to the type of secondary metal, oxide, or mineral present in the metallizing mixture. A tabulation was then made of the number of times each

additive to a refractory-metal base produced superior peel test values. Each additive was further weighted according to torque peel strength and whether it was used singly or in combination with another material. This technique produced numbers which could then be used to correlate the number of times strong seals were produced against the number of times each type of metallizing addition was tried. It was thus possible to determine the general effect of each additive to the refractory metal.

In addition, the total number of high peel test values was correlated against sintering temperatures in general, and against the alumina content of the body to which it was applied. Each metallizing composition and compositional type which produced a high seal strength was further examined to determine its optimum sintering temperature, the composition of the alumina body to which it best adheres, and the effect of concentration of the additive on seal strength.

(4) Torque Peel Test Results

The results of this analysis indicated that cerium oxide and thorium oxide additions to molybdenum produced the highest frequency of strong seals when used on Body AD-94. These were closely followed by additions of titanium and tungsten. In decreasing order of improved torque peel strength on AD-94 were additions to molybdenum of talc, manganese, sodium carbonate, titanium carbide, kaolin, and feldspar.* Pure molybdenum trioxide produced promising seals if considered only singly, especially at the lower sintering temperatures.

- - - - - - -

*The composition of talc is approximately $MgO \cdot SiO_2$, that of feldspar is $K_2O \cdot Al_2O_3 \cdot 6SiO_2$, and kaolin is $Al_2O_3 \cdot 2SiO_2 \cdot 2H_2O$.

Seal strengths were generally lower on Body AD-96 than on AD-94, with cerium oxide and thorium oxide producing good results. Feldspar, talc, titanium, zirconium, titanium carbide, kaolin, and silicon dioxide, in that approximate order, all produced promising seals. Pure molybdenum trioxide again rated fairly well if considered singly.

Seal strengths were much lower on Body AL-23 than on AD-94 or AD-96; feldspar, silica, and talc additions, however, appear to produce the best results. Barium oxide, calcium oxide, zirconium dioxide, and manganese also seemed to help. It is significant that silica and silica-bearing minerals appeared to produce the most satisfactory seals to AL-23, indicating that the formation of a silica glass or an alumina silicate compound in the metallizing layer or at the metallizing-ceramic interface may encourage high-strength seals to this high-alumina ceramic.

It is also interesting to note that feldspar and silica additions had the same approximate effect on seal strengths regardless of the choice of ceramic. This may occur because additional amounts of glassy phase over some optimum amount do not aid sealing, or because a chemical compound may be forming with the alumina. Talc produced stronger seals to the lower aluminas, possibly because of the silica contained in this mineral.

These ratings are mentioned in a general rather than a specific manner because of the many variables involved. Also, a composition will often yield a high torque peel value on a particular body at two widely separated sintering temperatures, but a low value when sintered to a temperature between them. In these cases, it is assumed that processing variables in plating, brazing, or testing affected the result;

this fact is considered in the evaluations. An example is Composition 24 in which the 1500°C torque peel results on AD-94 were considerably lower than the 1400°C and 1600°C values. Manganese dioxide, therefore, was considered slightly better for use in molybdenum on AD-94 than a numerical calculation indicated. This type of rating was considered satisfactory because its only function was to choose those mixtures to be considered for further testing.

Many trends were apparent when a careful analysis of adherence test and torque peel test data was made. For example, the silica and silicate additions, including feldspar and talc, yielded highest torque peel values when sintered at the higher temperatures. This suggested that migration of silicate glasses, the viscosity of which lowers with increasing temperature, may be responsible for stronger seals. A chemical compound might also be formed, and thus would be more complete at higher temperatures. Alternatively, the manganese compounds (for example, manganese dioxide in Compositions 23 and 24, and lithium manganate in Composition 88) yielded highest values when sintered in the lower range of temperatures investigated. The metallic additions to molybdenum, such as nickel, iron, cobalt, and tungsten, yielded highest strengths when sintered at the higher temperatures. With the exception of iron, which may oxidize under some sintering conditions, these additions, being soluble in molybdenum, may promote sintering and, thus, high seal strengths.

It can be seen that there was little difference whether the element titanium was added as metallic titanium or as the oxide (Compositions 32 and 33, respectively). This supported previous data that titanium oxidizes to titanium dioxide in wet cracked ammonia at elevated temperatures. Two additional observations were (1) small additions

of titanium or the oxide to molybdenum produced as good or better results as large additions and (2) these mixtures adhered better to the lower-alumina (94-percent Al_2O_3) than to the higher-alumina (99.6-percent Al_2O_3) ceramic. These observations suggested that the Glass Migration Theory rather than the Alumina Reaction Theory was operative. The same general observations are true for both manganese and manganese dioxide (Compositions 49 and 50).

The amount of titanium dioxide necessary to produce maximum strength appeared slightly higher than titanium metal; this was expected because the metal oxidized during sintering. Titanium also improved strength over a wide range, but smaller amounts were effective; an optimum addition appeared likely at about 3 percent by weight.

Additions of talc and feldspar also seemed to show an optimum strength at about 3 to 5 percent, though smaller amounts yielded higher strengths than pure molybdenum. Cerium oxide, though helpful over a wide range, apparently was best in small amounts, 0.5 percent yielding noticeably improved strengths.

Many materials appeared to improve adherence when added in very small amounts, but degraded seal strength when added in larger amounts. Barium oxide, lithium manganate, lithium titanate, and lithium carbonate showed this effect. Additions of metallic nickel and cobalt were also helpful when added in small amounts, less than 1 percent, but they degraded adherence when the concentration increased.

(5) Compression Test

The compression test was applied to the most promising compositions found by peel testing. Figure 4 illustrates the test specimens and fixture used. A 0.125-inch ceramic disc

was metallized on its outside diameter and then brazed into a tight-fitting Kovar sleeve to form a vacuum-tight assembly. This assembly was tested by compressing two 0.3125-inch tight-fitting rubber discs in the fixture. The loading rate used on the Baldwin Universal tester was 6000 pounds per minute to a load of 2000 pounds. The assembly was then checked again for vacuum tightness and loaded at a rate of 3000 pounds per minute in 400 pound increments, leak checking after each successive increment of load until a leak was detected. Of interest was an audible crack at failure, always detected while the specimen was being loaded, which allowed the operator to determine exactly when the leak occurred.

Results of the compression tests are shown in tables 9 through 13, which present data from metallized discs sintered at 1300°C, 1400°C, 1500°C, 1600°C, and 1700°C, respectively. The maximum load values recorded are slightly over 5000 pounds, indicated by the symbol $>$ 5000, because at that developed pressure the rubber discs flowed past the expanded Kovar sleeve in an almost liquid condition. Later tests were limited to 4000 pounds since the rubber distorted and shredded. Figure 5 shows a section of two assemblies which would not fail even after a loading of $>$ 5000 pounds. These assemblies, though distorted, are still vacuum tight.

(6) Compression Test Results

It can be seen from table 8 that only two mixtures, Composition 50 and Composition 199, showed promise of high-strength seals when sintered to 1300°C. Composition 50 is a molybdenum-manganese mixture with an addition of silica, and Composition 199 is a 100-percent molybdic trioxide mixture.

Many more metallizing compositions yielded promising ceramic-to-metal seal strengths when sintered at 1400°C, as indicated by the compression values shown in table 9. For example, Composition 43 with an addition of feldspar and Composition 45 with an addition of talc produced fairly high-compression values on high-alumina AL-23. Glassy phase resulting from diffusion of these silicate materials may be instrumental in the sealing of the materials. Composition 47 with silica and MnO incorporated in the mixture and Composition 50 with silica and manganese showed promising results at this sintering temperature.

A general summary of the compression test data for approximately 1500 test specimens is shown in table 14. The type of mixture which produced the highest seal strengths, along with symbols which represent metallizing systems, are presented. Where two or more compositions were formulated within a given system, some using the metal and others using the oxide, only the metallic symbol describes the system. Where only the oxide was used, it is so written. The figure of merit represents the number of times any metallizing system produced strong seals as opposed to the number of mixtures which were formulated and tried on the system. For example, if five cerium oxide and molybdenum mixtures were tested and four were associated with strong seals, the figure of merit would be 4/5. In general, strong seals are defined as those which are equal or superior to the strength which would be generated using a 20-percent manganese, 80-percent molybdenum metallizing mixture. Many attempted metallizing systems failed to produce strong seals, resulting in a figure of merit of 0/4, for example; these are not included in the table.

Several observations can be made by studying table 14. One of the most important is that a very large number of metals or oxides can be added to molybdenum to produce satisfactory ceramic-to-metal seals. No fewer than 16 metals or their oxides were found to produce seals of the same or higher quality as manganese.

An immediate observation can also be made regarding the sharp decrease in metallizing systems which were satisfactory on the higher-alumina ceramics, as compared with the 94-percent alumina body. The increased difficulty in sealing to high alumina is thus apparent in most metallizing systems, and not only in the molybdenum-manganese systems as has been generally conceded in the industry.

To accomplish seals to the 99.6-percent alumina ceramic, AL-23, silica additives, at 1400°C and 1500°C, were suitable in a large percentage of cases. Examples of this are Compositions R39 and R50, which showed higher strengths to the AL-23 body than to the lower-alumina Coors ceramics. At 1600°C and 1700°C, titanium additives and molybdenum and glass additions were most satisfactory. Very few promising metallizing mixtures were generated at 1300°C, but the number increased steadily to 1600°C and then decreased at 1700°C.

As the sintering temperature was increased, a steady decline was noted in the number of metallizing mixtures containing manganese. At 1400°C, on Coors AD-94 and AD-96, all but one composition were manganese bearing, at 1700°C, none contained manganese. This decrease also occurred between 1500°C and 1600°C.

Titanium was a material very frequently associated with high seal strength. At 1400°C, slightly less than one

third of the high-strength compositions contained titanium or titanium dioxide; at 1500°C, more than half did. The percentage indicated a marked decrease, however, at 1600°C and 1700°C.

Materials which were added solely to promote molybdenum sintering were found frequently at 1600°C and 1700°C. These are metals such as iron, nickel, cobalt, and tungsten which will remain in the metallic state in a wet cracked ammonia atmosphere. As shown by the figures of merit, nearly 40 percent of the compositions at 1600°C contained sintering promoters and nearly 60 percent did so at 1700°C. The balance of suitable mixtures at these temperatures was rather random, with silica additions being the most common.

Pure molybdenum and molybdenum oxide made many satisfactory seals. The oxide was promising at 1300°C and 1400°C, whereas pure molybdenum worked well at 1600°C and 1700°C. Oxides other than molybdenum oxide did not offer any measurable advantage over pure metallic additions, undoubtedly because the metals quickly developed their stable oxidation levels anyway with cracked ammonia atmospheres.

(7) Tensile Test

Those combinations of experimental metallizing mixtures, ceramic bodies, and sintering temperatures that yielded the highest values in the compression test were chosen for tensile testing. Sperry Tensile Design No. 1 (figure 6a) was used for the tensile tests. Because of the variation between the three specimens of each combination and because of the general decrease in strength noted with the higher alumina bodies, tensile tests were conducted on combinations yielding the following or higher compression test values:

	AD-94	AD-96	AL-23
Compositions having individual load values of	5000 lb	3500 lb	3000 lb
Compositions having average load values of	3000 lb	2500 lb	2000 lb

After cleaning and air firing the tensile specimens, two coats of a metallizing mixture were hand painted on the ceramic surface, each coat being sintered at the appropriate temperature. Each metallized surface was then hard nickel plated. Two half specimens were then brazed together using OFHC copper shim stock in a suitable brazing jig. Tensile testing was done on a Baldwin Universal Tester (60,000-pound capacity), using a load rate of 3000 pounds per minute. Rubber gaskets between the surface of the ceramic and the steel pulling fixtures were used to equalize the stresses at the shoulder of the tensile specimen. Tensile testing data are shown in tables 15 through 19, for specimens sintered at 1300°C, 1400°C, 1500°C, 1600°C, and 1700°C, respectively.

(8) Tensile Test Results

It is apparent from the tables that some combinations yielded tensil values in excess of the 25,000-psi goal of this study. All tensile test values were corrected for the bending moment induced by the nonlinear loading, as discussed in paragraph 6 of this report. Composition 65 on Body AD-94 at a 1500°C sintering temperature, for example, yielded one tensile test value of 28,400 psi, with an average tensile value for three duplicate speciments of 21,400 psi. As shown in figure 7 it is the ceramic which fractures in the vicinity of the seal area, but not through it, for these higher-strength ceramic-to-metal seals. Left to right, figure 7

illustrates a specimen of AD-94 metallized with Composition 65, yielding a tensile strength of 28,400 psi; a specimen of AD-96 metallized with Composition 72, yielding a tensile strength of 22,000 psi; and a specimen of AL-23 metallized with Composition 50, yielding a tensile strength of 16,100 psi. In each case the sintering temperature was 1500°C.

It should be noted that the appearance of the fracture is not the most reliable means for determining if the seal is stronger than the ceramic. The AD-94 specimen which failed at 28,400 psi shows a failure largely in the seal area. However, the AL-23 specimen definitely has a seal stronger than the ceramic, although it failed at 16,000 psi. The contribution of thermal-mismatch stress of the solder itself will undoubtedly affect the physical nature of the failure. This is an area in which more knowledge is needed. It is of interest that in over 400 tensile pulls only one case of shoulder fracture is encountered.

The analysis of the tensile test data was conducted by using the same techniques applied to the compression test data, as described in paragraph 2b(6). Table 20 shows the metallizing systems which produced the strongest seals. As was the case for the compression test results, one notices immediately the wide variety of compositional systems which produced strong seals, as well as the sharp decrease of compositions which were suitable for the 96-percent and the 99.6-percent aluminas.

Compositions containing manganese predominated at 1300°C and 1400°C. At 1500°C, manganese-bearing compositions decreased sharply, with two of six superior compositions containing manganese. At 1600°C and 1700°C, only one composition contained manganese.

All satisfactory seals to AL-23 contained silica and, in most cases, manganese. These seals were sintered at 1300°C, 1400°C and 1500°C. No strong seals were made at 1600°C and 1700°C to AL-23, although several compositions were attempted.

Titanium did not produce superior seals as often when using the tensile test as it did with the compression test. These compositions also predominated at lower temperatures. At 1600°C and 1700°C, there was only one superior titanium-bearing composition.

The wide variety of compositional systems at 1600°C and 1700°C is rather difficult to understand. At these temperatures, 8 out of 26 compositions contain a sintering promoter as the only molybdenum addition. Silica was present in another five compositions. The remaining compositions consisted of additions of thoria, zinc, titanium, ceria, zirconia, and manganese, as well as pure molybdenum. No significance in this list could be found, except to note the variety involved. A check on each composition involved, however, showed that none of these metallic additions was in excess of 15 percent by weight.

(9) Final Observations

Final observations in this phase of the study program should be made by referring to table 21. The seven most promising compositions and their sintering temperatures are shown for the three bodies studied. The best values for AD-94 were obtained using Composition 65, a 2.5-percent titanium addition to pure molybdenum.

The tensile test average is 21,400 psi. Both Compositions 91 and 141 produced averages over 15,000 psi. One basic formulation, molybdenum-silica-manganese, was excellent

on AL-23 and AD-96. Molybdenum-ceria also produced high-strength seals to AD-96. All seven compositions shown in table 21 are extremely promising and an investigation of their reliability is highly desirable.

5. PHASE III - BRAZING INVESTIGATION

The brazing of ceramic-to-metal seals is recognized as paramount in achieving reliable and strong seals. Factors such as joint clearance, solder type, and soak time and rate, to name a few, have been established as important variables. Although a study of this phase was planned, it was found that seals can be made as strong as the ceramic by using standard Sperry brazing techniques, provided a superior metallizing mixture was properly sintered onto the particular ceramic considered.

6. PHASE IV - TESTING INVESTIGATION

a. Comparison of Test Methods

An accurate and thorough testing endeavor was necessary for the proper evaluation of this program, because the value of the data obtained was to be determined largely by the test pieces and test methods selected. Such a program, with emphasis on reproducibility, was therefore conducted by evaluating the tensile, the compression, the torque peel, and the drum peel tests. Sixty-two ASTM tensile test specimens were prepared. These, in addition to the two half specimens bonded together, had two Kovar strips bonded to the flat surface of one of the halves to measure torque peel, and two preformed Kovar strips sealed to the outside diameter of each of the two shoulders to measure drum peel. All brazes were

made simultaneously, producing the specimens shown in figure 8. The ceramic used was Coors AD-94, metallized with an 80-percent molybdenum, 20-percent manganese mixture, sintered at 1500°C, plated with hard nickel, and brazed using OFHC copper shim stock.

Torque peel data were evaluated by inserting the specimen into the fixture shown in figure 3. Flat Kovar strips were crimped and engaged into a slot built in the cylinder of the test fixture as shown. The load in inch-pounds was read on the torque wrench by the operator, who recorded the maximum value indicated.

The drum peel test was chosen to eliminate the operator variables in rate of application of the load and in the reading of the data. Figure 9 illustrates the fixture used. The load was applied at a constant, reproducible rate and recorded as pounds pulled versus time on strip chart paper. Figure 6b is an example of the tensile specimens of the design of which was originally proposed by ASTM. The method used was that under discussion by Group V-D, Subcommittee F-1 of that organization.

To evaluate seal strength by compression testing, a specimen and a fixture as shown in figure 4 are used. This test has a distinct advantage in that the configuration of the test specimen closely resembles the geometry often used in tubes. Compressive forces loaded at a prescribed rate to the ends of the fixture produce hydrostatic forces in the rubber discs, these forces tear the ceramic from the Kovar sleeve. Failure is defined as the load at which the assembly is no longer vacuum tight.

Twenty-five comparison specimens for compression testing were prepared from Coors AD-94 ceramic, Kovar metal,

and the 80-20 molybdenum-manganese metallizing mixture. These were sintered at 1500°C, nickel plated, and OFHC copper brazed. Results of the test comparison series are listed in table 22, which shows an average strength value, the standard deviation, the coefficient of variation, and the number of trials for each compression, tensile, drum peel, and torque peel test.

It can be seen in table 22a that the compression test, with a coefficient of variation of only 10.5 percent, had the greatest reproducibility and least variation. The tensile test with a coefficient of variation of 27.8 percent proved to be less reproducible than the compression test. The torque peel is significantly more reproducible than the drum peel test and therefore was chosen for the initial evaluation of the 200 experimental metallizing mixtures prepared later.

Table 22b presents a similar comparison in which n, the number of trials, was in all cases equal to 25. The most significant improvement was in the torque peel test, indicating it was the most sensitive to changes in brazing conditions and also suggesting it would be the most sensitive to variations in seal strength.

The averages in table 22a tend to indicate that the following measures of seal strength are equivalent for the particular ceramic, metallizing mixture, and conditions studied:

- Tensile Test 2011-lb load, 11,061 psi
- Compression Test 2428-lb load
- Drum Peel Test 8.08-lb load
- Torque Peel Test 2.85-in.-lb torque

On the basis of the above single-point curves, a linear extrapolation suggests that the following values are equivalent to a 25,000-psi tensile strength:

- Compression Test 5200 pounds
- Drum Peel Load 17.25 pounds
- Torque Peel 6.13 inch-pounds

As previously mentioned, a limitation was found in the compression test in that in pressures above a 5000-pound load the rubber discs flowed in an almost liquid condition past the expanded Kovar sleeves.

b. Tensile Test Specimen Design

During the course of this investigation it was found that the tensile test specimen now under consideration by ASTM (figure 6b) had a serious shortcoming for the measurement of very strong ceramic-to-metal seals. This fault is that failures occurred at the shoulder rather than in the seal area. ASTM, in efforts to eliminate this fault, has considered an increase in fracture path, as shown in figure 6c. The calculations presented in the Third Technical Note[1] indicated that an increase in the radius of curvature at the shoulder should decrease stresses in that area[27]. Because it was necessary to make certain assumptions between the case cited by Timoshenko and the one in question, it was decided to measure the exact stress picture using the photoelastic technique.

c. Photoelastic Study

Full-scale models of the three designs in question were made of a standard photoelastic material, as described in the Fourth Technical Note[1]. By stressing models at elevated temperatures and chilling them while still stressed, the

stresses produced in a three-dimensional object can be viewed by carefully sectioning and polishing the object after it has cooled to room temperature. A photograph of a flat slice of each of the three specimens with the stress pattern "locked in" is shown in figure 10. The specimens are, left to right, Sperry Tensile Design No. 1 (designed under this contract), ASTM Tensile Design No. 2, and the design under present use by ASTM.

The fringes visible in the ASTM sample show that there is a higher level of stress in the shoulder than in the seal area by a ratio of approximately 2.5 to 2.0, thus predicting failure in the shoulder area. Design No. 2 shows approximately equal stress in both the shoulder area and the seal area, so a failure at either point is equally probable. Sperry Design No. 1, however, shows a greater tensile stress at the seal area than at any other point and thus should fail at the seal.

The photoelastic study revealed another characteristic of these specimens which was not suspected previously. The bending moment induced by loading which was not directly above the fracture area gave rise to nonuniform tensile loading in that area. This was a significant discovery because it meant that all tensile values measured to date were actually higher than a straight-forward calculation would indicate. Additional tensile stresses on the outside surface of the specimen and compressing stresses on the inside were caused by the bending moment. This changed the stress distribution from that of pure tensile stress to that of a combined tensile and bending stress.

Careful analysis of the stress pattern allowed the calculation of this maximum combined stress, presented in the

Fourth Technical Note. Based on the assumption that the bending stress varied uniformly across the section, a maximum combined stress in Sperry Tensile Design No. 1 was calculated to be 1.33 times the direct tensile stress. Similar values for the ASTM standard specimen and ASTM's Design No. 2 were 1.09 and 1.18, respectively.

It can be concluded that the ASTM specimens give unreliable results when shoulder breaks occur because of the stress concentrations in the shoulders. Design No. 1 is the preferred specimen from this point of view. All three specimens showed undesirable bending effects which cause tested tensile specimens to fail at lower than true tensile values by the amounts calculated. It may be possible to eliminate this effect by redesigning the specimen so that the center of the seal area and the point of loading are colinear. For the present program, more realistic tensile strength values were obtained by multiplying the tested value by the calculated factors.

d. One-Piece Test Specimens

For further evidence that the foregoing calculations and observations were correct, the two new tensile specimens (figure 6a and 6c) were manufactured into one-piece test specimens; tensile testing would thus reveal the location and magnitude of the fracture. As illustrated in figure 11, Sperry Tensile Design No. 1 fractured at the desired location whereas Design No. 2 did not. An average of four replica specimens of each body produced the average values shown on the following page. It should be noted that these figures include the correction factor due to the bending moment inducted by nonlinear loading.

Tensile Specimen	Average PSI
Sperry Design No. 1	25,300
ASTM Design No. 2	16,000

e. Tensile Specimen Gasket Materials

A series of tensile tests was conducted to compare soft lead and rubber gaskets for use between the shoulders of tensile specimens and the steel pulling grips. No differences in tensile values were found; therefore, rubber gaskets were used because of the greater simplicity of assembly.

7. PHASE V - TEMPERATURE INVESTIGATION

Because of the vast quantity of work necessary to complete Phases II and IV, the metallizing and testing investigations, time and funds were not available to conduct a major effort in this phase. This is a recommended area for future study.

8. PHASE VI - STRESS INVESTIGATION

a. Introduction

The importance of stresses in ceramic-to-metal seals is generally acknowledged by all who have become involved in seal design, manufacture, or application. Distinctly different characteristics prevail for electrical ceramics and the wide variety of metals to which they may be sealed. Because of these differences, in particular their thermal expansion and ductility properties, substantial stress is known to exist when a brazed seal is cooled to room temperature. Although design techniques are known to circumvent these residual stresses, virtually nothing of a quantitative nature is known.

Considerable work has been done on stresses present in glass-to-metal seals, enamel coatings, etc. However, no published papers could be found regarding stresses in ceramic-to-metal seals.

It was the goal of this phase to discover more about the nature of seal stresses. In particular, it was hoped that seal stresses could be calculated, knowing enough about the materials involved. This goal has been realized. More basically, it appears that stress constants can be calculated, not only for ceramic-to-metal seals, but also for any two, brazed materials having different properties.

b. Theory

Consider an infinitely small seal element as shown in figure 12a prior to brazing. Imagine the top cube to be the higher expanding member and δ to be the total expansion mismatch in inches per inch. Assume, for the initial arguments, that the bottom member is totally unyielding and does not expand. When the system is heated, the configuration shown in figure 12b is realized. The seal is thus achieved and the system is allowed to cool, resulting in the configuration shown in figure 12c. Considering a single plane in the element, illustrated by figure 12d, the distance δ is also equal to the total strain developed in the cooling process; this is a key point in the argument.

The acceptance of the preceding argument, equating thermal expansion mismatch to total strain, provides the first means for the calculation of seal stresses.

Imagine that the thermal expansion mismatch between the top and, for the moment, the nonexpanding bottom member, as shown in figure 13a, is the distance δ in inches per inch

at the temperature at which the solder melts. Because δ is also equal to total strain, it can be transposed to a stress-strain curve as shown in figure 13b. The stress level can then be read directly from the ordinate. If the stress generated exceeds the yield point of the metal, the procedure does not change, but will result in a transposition such as figure 13c illustrates.

A correct stress determination at the seal interface would result from the foregoing procedures if (1) the bottom member were nonexpanding and nonyielding and (2) a single stress-strain curve were operative at all temperatures. Neither is the case.

The actual, final configuration of the element in question would be as shown in figure 14a. The top member would be pulled into tension and the bottom into compression. Defining tension as positive strain and compression as negative strain, both can be plotted using the same ordinate, as shown in figure 14b. Thermal expansion mismatch can then be measured as shown in figure 14c and transposed to produce a somewhat lower stress, for a fixed δ, than would be the case neglecting the lower expanding member.

The problem of changes in the stress-strain curve with changing temperature presents a somewhat more difficult situation. A different curve would be operative at any temperature, and a solid surface could actually be generated for the three-component system: stress-strain-temperature. If the equation of such a surface could be determined, a mathematical solution could be achieved by integrating the stress-rate curve. Such a procedure would be extremely difficult, probably resulting in a machine calculation. A simpler graphical approximation is preferred, as described in the following paragraphs.

Assume that the ceramic member expands, but that it is totally nonyielding. Such an assumption could be circumvented, as previously described, by plotting negative strain. Even in actual measurements, however, the yield contribution of the ceramic can be shown to be so small that its neglect produces virtually no error.

Consider a family of stress-strain curves, as shown in figure 15a, in which virtually no stress could be developed regardless of strain at temperatures down to 500°C, and then suddenly the room-temperature curve became operative. The result would be that only the strain or thermal mismatch developing from 500°C to room temperature would be of importance, and the mismatch in this temperature range could be transposed, as previously discussed.

Next, consider a family of stress-strain curves in which a measurable curve is operative from braze temperature to 500°C, and then suddenly a second curve becomes operative for all temperatures between 500°C and room temperature. This system is shown in figure 15b. The transposition can then be carried out by using the 500°C to braze temperature thermal-expansion mismatch. If no further temperature drop were experienced, the stress level would be determined. At 499°C, however, the second curve would become operative. Stress level would not have changed substantially from 500°C to 499°C, only the curve which is operative; one would begin to accumulate stress on a new curve beginning from point A. From point A, the thermal mismatch from 500°C to room temperature is again transposed to determine the final stress level. This procedure can be applied to approximate the final stress level, providing the necessary curves are available. The accuracy increases with the number of curves; in this study four curves were found to be quite satisfactory.

One basic observation should be made at this point. A seal stress thus determined and existing at the seal interface is a constant value for any two materials for a given braze temperature. It is not geometrically sensitive at the interface, and operates equally in any direction in the seal plane. However, at any point above the interface, the stress will be influenced by the geometry of the seal; factors such as bending in butt seals may interrupt its normal development. In the experimental study of these stresses, samples were used which developed stress uniformly about an axis. The experimental evidence in support of these theories demonstrates excellent agreement.

c. Experimental Procedure

To investigate the preceding theory required experimental testing in two distinct areas. One was the development of stress-strain curves at elevated temperatures for the same metals, and at annealing temperatures used for making seals. The second was the fabrication of seals in which the stress could be measured by strain gages. For the second area, the technique was to apply the gages to the metal member, remove the ceramic, and measure the metal relaxation or strain which took place. This provided sufficient data to enable a comparison of calculated stress with measured stress.

The metals chosen for the study were 303 stainless steel and "A" grade nickel. The stainless steel was selected because of its high-temperature strength and nickel because of the reverse tendency. Copper solder was chosen because of its ease in acid removal and generally common usage.

(1) Stress-Strain Measurements

Considerable data can be found in the literature regarding the high-temperature characteristics of nickel and stainless steel. The data presented some difficulty in that it was not available for the same annealing times and temperatures which would be experienced in brazing. In addition, heating rates were different. For these reasons, precise measurements were made after the metal was exposed to the brazing cycle used in making the seals.

The initial plan was to machine stress-strain specimens from the same tubular stock from which the seal metals were to be fabricated. It became apparent, however, that several problems were involved with this procedure. Fabrication of the specimens provided the first difficulty. The stock had to be cut and rolled flat, requiring high pressures. Because of spring-back, the pieces had a low residual curvature. A similar shaped mold had to be formed to overbend the pieces. Secondly, considerable cold working was introduced which could be removed only by undesirable annealing. Finally, the samples thus produced showed poor stress-strain repeatability.

Because of these problems it was decided to machine specimens from sheet stock, which, upon checking, was found to have virtually the same hardness as the metal stock to be used for seals. Exact discussions of the hardness of the metal, the rolling and machining technique, and the specimen design can be found in the Second and Third Technical Notes[1].

The specimens, after being passed through the brazing furnace, were placed in a high-temperature extensometer, as shown in figure 16. Preliminary test runs were made to test the equipment, and the technique was refined.

(2) Seal Residual Stress Measurements

Because of ease of calculations and to achieve uniform stress distribution, a test specimen with a design as shown in figure 17 was chosen. The small shoulder on the inside diameter of the metal was provided for placement of solder. A wall thickness of 0.100 inch was used for the stainless seal and a wall thickness of 0.080 inch for the nickel seal. The differences developed because of stock availability. These can be easily taken care of mathematically as shown in paragraph 8c(2). Samples were brazed using OFHC copper solder.

Five resistance-wire strain gages were bonded to the outer circumference of the metal, three to measure tangential strain and two to measure axial strain, as shown in figure 17. The sample was fitted with a collar equipped with terminals. Lead wires from the gages were attached to the terminals, which in turn were equipped with lead wires to the measuring bridge circuit. An instrumented sample is shown in figure 18.

Solder removal was accomplished by leaching out the solder with a 25-percent ammonium persulfate solution at 120°F. Using a jeweler's saw to remove the solder and direct axial loading to remove the ceramics were considered. These techniques were abandoned, however, when early trials showed the leaching technique to be the most promising.

To facilitate exposure of the solder to the ammonium persulfate without attacking the gages, a closed circulatory system was developed. Samples were provided with teflon-gasketed aluminum caps through which the leaching compound could be circulated. A bank of four specimens was then set

up and ammonium persulfate was drawn through the system in series (figure 19). It was found highly desirable to generate a mild negative pressure within the circulatory system, thus greatly reducing leaks. This was accomplished by pulling rather than pushing the ammonium persulfate through the system. Gage readings were taken continuously during the leaching process. The solder was completely removed in about 10 hours for the nickel and in about 24 hours for the stainless steel.

(3) Calculations

In the previously discussed theory, a method for calculating stresses at the seal interface was described. Experimental procedures allowed measuring the actual tangential stress on the outer circumferential face of the metal. To calculate the stress from the inner face to the outer face, formulas which are available in the literature can be used[28].

$$S_t = \frac{P_i r_i^2}{r_o^2 - r_i^2} \left[1 + \frac{r_o^2}{r^2} \right]$$

where

S_t = tangential unit stress at radius r

r = any radius

P_i = internal radial pressure

r_o = outside radius

r_i = inside radius

For the special case where

S_{t_o} = tangential stress on outside surface

S_{t_i} = tangential stress on inside surface

it can be shown that

$$S_{t_o} = \frac{2\, S_{t_i}\, r_i^2}{r_o^2 + r_i^2}$$

This expression can then be used to calculate the outside tangential stress using the value predicted for inside tangential stress as discussed previously. A comparison between measured and calculated stresses can then be made.

One final consideration remains. Because the elastic limit of the metal will have been exceeded when brazing, residual stresses can be expected in the metal ring despite the fact that the ceramic has been removed. This condition does not invalidate the use of the above formula, because, in solder removal, unloading will then take place according to Hooke's Law[29]. Simply, more stress relief can be accomplished by machining the inside diameter of the metal ring.

d. Experimental Results

The results of the stress-strain measurements are shown in figures 20 and 21 for the nickel and 303 stainless steel, respectively. Thermal expansion curves which were used are illustrated in figure 22. Table 23 shows the results of measured as well as calculated stress. Outside tangential stress is designated by the symbol S_{t_o}, and outside axial stress by S_{a_o}. It should be noted that no means could be found to calculate S_{a_o} from the inside face to enable a comparison with measured values. The inside tangential stress or brazing constant K, calculated as previously described, represents a stress in any direction within the seal plane. Although approximately 15 samples were made in each metal,

time was available to measure only 4 of each; these were chosen at random. Sample dimensions and physical constants used in the calculations are as follows:

Young's modulus for nickel = 30×10^6 psi/in./in.

Young's modulus for 303 stainless steel = 29×10^6 psi/in./i

Ceramic O.D. = 1.577 inches

Nickel O.D. before braze = 1.743 inches

Nickel O.D. after braze = 1.765 inches

Stainless steel O.D. before braze = 1.783 inches

Stainless steel O.D. after braze = 1.803 inches

e. Summary of Stress Study

A study of table 22 shows excellent theoretical and experimental agreement within the limits of the testing techniques. It appears that a stress constant does exist in brazing ceramic-to-metal seals and that it can be used in calculating seal stresses. The implications of these findings are noteworthy. Tables of stress constants could be generated for combinations of materials at various temperatures. The first means would thus be provided for the calculation of previously undeterminable stresses. Thus, a method would be available to enable the choice of low stress combinations as well as the ability of making use of prestressed geometries or structures.

SECTION C

CONCLUSIONS

9. CONCLUSIONS

The following can be drawn from the data presented:

a. Ceramic-to-metal seal strengths as high as 28,000 psi in tension were found for the 94-percent alumina body. The maximum strengths decreased - as the alumina content of the ceramic member increased - to 22,000 psi in tension for the 96-percent alumina body and to 16,100 psi for the 99.6-percent body. Sealing techniques were developed which produce seals as strong as the ceramic.

b. The optimum sintering temperatures vary with the particular metallizing mixture under consideration; however, in most cases, these were in the 1500°C to 1600°C sintering-temperature range.

c. At the lowest sintering temperatures (1300°C and 1400°C), the strongest seals resulted from straight molybdic trioxide metallizing mixtures or molybdenum-mangangese base mixtures with additions of silica or titanium helpful. Molybdenum-manganese mixtures were less frequently associated with high-strength seals at 1500°C. Additions of titanium and ceria to pure molybdenum were stronger after sintering at this temperature. At highest sintering temperatures (1600°C and 1700°C), those additives which promoted molybdenum sintering generally yielded the highest seal strengths.

d. Metallizing compositions for AL-23, a 99.6-percent alumina ceramic, almost invariably required silica or silicate-bearing minerals such as feldspar or talc to yield strong ceramic-to-metal seals.

e. A photoelastic study of the tensile test specimens disclosed and allowed the calculation of bending moment forces in the seal area due to nonlinear loading. In addition, the stress concentrations which can cause shoulder breaks are now well understood.

f. A tensile test design was developed in which shoulder breaks, even in ultra-high-strength ceramic-to-metal seals, are no longer a problem. Only one shoulder break was encountered in over 400 fabricated and tested asemblies.

g. A basic investigation of ceramic-to-metal seal stress developed a method for solder removal, thereby enabling accurate stress measurements. Theoretical work indicates that a brazing stress constant exists which can be calculated and used for the correct determination of seal stresses, not only for ceramic-to-metal seals, but also for any two dissimilar materials brazed together. Experimental data in support of the brazing-constant theory demonstrated excellent agreement.

h. The results of this investigation support, in general, the Glass Migration Theory of adherence.

SECTION D

RECOMMENDATIONS

10. RECOMMENDATIONS FOR FUTURE WORK

Seal reliability, using the improved sealing compositions developed under this contract, should be studied. This should include the importance of minor and major changes in processing variables including a wide range of factors, such as furnace atmosphere, metallizing thickness, sintering time and temperature, plating thickness, and brazing procedures. Criteria should be established to bracket the maximum variation which can be tolerated in these areas. Work is also recommended to determine the compatibility of the metallizing procedures for tube usage. Factors such as outgassing, cathode poisoning, life, thermal cycling, and r-f characteristics require study.

Of equal importance is the study of leak path. The mechanism of leaks, their origin, and elimination require immediate study and understanding.

Long-range studies are required in the areas of ceramic-to-metal seal adherence, particularly where 100-percent aluminas are involved. When the sealing of materials other than alumina is considered, large savings in engineering, manpower, and money can be realized if complete understanding of adherence mechanism is available.

The investigation of stresses should be continued. With the mechanics of stress calculation now available, work should be initiated to determine the brazing constant for large numbers of materials.

Additional work on the ceramic itself should be considered in long-range thinking. This should include the use of beryllia ceramics. The creation of higher-strength, lower-loss ceramics should be encouraged. Basic understanding of electrical-loss characteristics in the various solid and liquid phases in the ceramic is important.

In general, efforts should be made to keep the development of ceramic and ceramic-sealing technology at the same level as tube technology.

BIBLIOGRAPHY

1. Metal-to-Ceramic Seal Technology Study, First through Fourth Technical Notes, RADC-TN-59-370, RADC-TN-60-53, RADC-TN-60-108, RADC-TN-60-192, furnished by Sperry Gyroscope Company to U.S. Air Force under Contract No. AF 30(602)2047.

2. Kohl, W., "Electron Tubes For Critical Environments", WADC-TR 57-434, March 1958.

3. Van Houten, G., "A Survey of Ceramic-to-Metal Bonding", American Ceramic Society Bulletin, Vol. 38, June 1959, pp. 305-307.

4. Pulfrich, H., U.S. Patent 2,163,407 (1939).

5. Pulfrich, H., U.S. Patent 2,163,408 (1939).

6. Pulfrich, H., U.S. Patent 2,163,409 (1939).

7. Pulfrich, H., U.S. Patent 2,163,410 (1939).

8. Jenkins, D., "Ceramic-to-Metal Sealing; Its Development and Use in the American Radio Valve Industry", Electronic Engineering, London, Vol. 27, July 1944, pp. 390-394.

9. Pulfrich, H., U.S. Patent 2,174,390 (1940).

10. Pulfrich, H., German Patent 659,427 (1938).

11. Vatter, H., "On the History of Ceramic-to-Metal Sealing Techniques", Vol. 4, February 1956.

12. Vatter, H., German Patent 645,871 (1935).

13. Vatter, H., German Patent 682,962 (1939).

14. Vatter, H., German Patent 689,504 (1938).

15. Vatter, H., German Patent 706,045 (1938).

16. Vatter, H., German Patent 720,064 (1936).

17. Pincus, A., "Metallographic Examination of Ceramic-to-Metal Seals", J. Am. Ceram. Soc., Vol. 36, May 1953, pp. 152-158.

18. Pincus, A., "Mechanism of Ceramic-to-Metal Adherence", Ceramic Age, March 1954, pp. 16-20, 30-32.

19. Armour Research Foundation, Illinois Institute of Technology, "Literature Review and Industrial Survey of Brazing", Final Report, Project No. 90-1060B for Frankford Arsenal.

20. Gulbransen and Wysong, "Thin Oxide Films on Molybdenum", A.I.M.M.E. (Metals Tech) 14 T.P. No. 2226, 1-17, September 1947.

21. Dushman, S., Scientific Foundations of Vacuum Technique, New York, John Wiley & Sons, 1949.

22. Kubaschewski and Evans, Metallurgical Thermochemistry, Pergamon Press, 1958, Table E.

23. Coughlin, J., Contributions to the Data on Theoretical Metallurgy (XII Heats and Free Energies of Formation of Inorganic Oxides), Bulletin 542, Bureau of Mines, pp. 23, 31.

24. Denton, E.P. and Rawson, H., "The Metallizing of High Alumina Ceramics", Brit. Ceram. Soc. Trans., 1960, pp. 25-37.

25. Cole, S.S. and Hynes, F.J., "Some Parameters Affecting Ceramic-to-Metal Seal Strength of a High Alumina Body", Bul. Am. Ceram. Soc., Vol. 37, No. 3. 1958, pp. 135-138.

26. American Society for Metals, Metals Handbook, ASM, 1948, pp. 1146-1240.

27. Timoshenko, and MacCullough, Elements of Strength of Materials, New York, D. Van Nostrand Co., Third Edition, June 1949, pp. 25-26.

28. Timoshenko, Strength of Materials, Part II, "Advanced Theory and Problems", New York, D. Van Nostrand, p. 211.

29. Ibid, p. 389.

APPENDIX

TABLES

TABLE 1

SUMMARY OF THERMODYNAMIC CALCULATIONS

Metal	Reaction In Wet H_2	Melting Temperature of Metal (°C)	Melting Temperature of Oxide (°C)	Eutectic Between Oxide and Al_2O_3 (°C)
Ti	Oxidises	1800	2130	1715
Ba	Oxidises	850	1920	1660
Ca	Oxidises	810	2570	1400
Co	Reduces	1480	1800	1650
Mg	Oxidises	650	2800	1900
Si	Reduces	1450		No Reaction
Pb	Reduces	327	880	No Reaction
Si	Oxidises	1420	1710	1995
Sr	Oxidises	800	2430	1800
Th	Oxidises	1840	2800	1400
Zn	Oxidises	419	1800	1700
Zr	Oxidises	1700	2700	1700
Cu	Reduces	1088	1235	1200
Mn	Oxidises	1260	1780	1520
Fe	Dew Point Sensitive	1500	1500	1300

TABLE 2

RESULTS OF ADHERENCE TESTS AND TORQUE PEEL TESTS PERFORMED ON SPECIMENS METALLIZED WITH COMPOSITIONS BASED ON THE ALUMINA REACTION THEORY

Composition Number	Composition and Weight (gr)	Sintering Temp. (°C)	Adherence Rating* AD-94	AD-96	AL-23	Torque Peel Value** AD-94	AD-96	AL-23
1	210 Mo 100 BaO	1500 1600 1700	P P P F FF P FF FF P	0 1/2 3/4	0 1/2 1/2	3/4 1/2 1/2
2	210 Mo 126 CaO	1300 1400 1500	P P P F F G G G G	1/2 0 2	3/4 0 2	0 0 1 1/2
3	210 Mo 90 Mg	1500 1600 1700	P P P F P P G G F	1/2 2 1	0 3/4 1 1/4	3/4 1/4 0
4	210 Mo 150 MgO	1500 1600 1700	G G F FG FG FF G F F	2 1 2 1/2	1 3/4	0 1/2 0
5	210 Mo 193 SiO_2	1400 1500 1600	FF F F F F G F F FG	0 0 3	0 0 1/4	3/4 1 1 1/4
6	255 Mo 96.5 SiO_2	1400 1500 1600	FF F G F F G F F FG	0 3/4 1 1/2	0 0 3/4	3/4 1 1/2 1 1/4
7	210 Mo 106 SrO	1500 1600 1700	P P P F P P FF FF P	1 3/4 2	1/2 1/2 1/2	0 3/4 0
8	210 Mo 102.5 ThO_2	1500 1600 1700	G P P G F FF G G P	1 1/2 4 5 1/2	1 3/4 2 1/2	0 1/2 0
9	210 Mo 90 Zn	1500 1600 1700	F P P FG F FF G FG P	3/4 3 1/2 5	1/2 1 1 1/4	0 1/2 0
10	210 Mo 112 ZnO	1500 1600 1700	F F P FG F FF G FG FF	3/4 1 1/2 3 1/2	1 1 1/2	0 0 0
11	210 Mo 121 ZrO_2	1500 1600 1700	G G FG G G FF G G G	1 1 2	1 1/2 1 1/2 2	0 3/4 1/2
12	255 Mo 50 BaO	1500 1600 1700	F P P G F FF G FF FF	1 1 2 1/2	1/2 3/4 1/2	1 0 1/4
13	255 Mo 63 CaO	1300 1400 1500	P P P FF P F G FG F	0 1 1/4	3/4 1/2 0 1	3/4 3/4 2 1/2
14	255 Mo 45 Mg	1500 1600 1700	P P P FF FF FF F FF	0 1 1/2	0 3/4 1/2	0 0 0
15	255 Mo 75 MgO	1500 1600 1700	G FG F G G F G G FF	1/2 1 1/2 5	3/4 3/4 2	0 0 0
16	255 Mo 53 SrO	1500 1600 1700	F P P F FF P G FF F	3/4 1 1/4 3/4	3/4 3/4 1/2	0 1/4 1/2
17	255 Mo 51 ThO_2	1500 1600 1700	G F P G G FF G G FF	1/2 5 1/2 3 1/2	3/4 3 1/2 3 1/2	0 1/4 1/2
18	255 Mo 46 Zr	1500 1600 1700	G F P G FG FF G G FG	1 1/4 4 5	3/4 1 1/2 2 1/2	0 1/4 1/2
19	255 Mo 56 ZnO	1500 1600 1700	F FF P G FG FF G G F	3/4 5 4 1/2	3/4 2 4	3/4 0 1/2
20	255 Mo 66 ZrO_2	1500 1600 1700	G G F G G FF G G FF	3/4 3 3/4	3/4 3 1/2 3	1 1/4 0
21	255 Mo 45 Mn	1400 1500 1600	G FG F G FG F G G FF	3 1/2 3/4 3	7/8 1/2 5/8	3/4 1 5/8
22	210 Mo 90 Mn	1400 1500 1600	G G F G FG F G G FF	3/4 1 3/4	3/4 3/4 1	1/2 3/4 0
23	210 142 MnO_2	1400 1500 1600	FG FG F G FG F G G FF	2 1/2 2 1	1 1 3/4	3/4 1 1
24	255 Mo 71 MnO_2	1400 1500 1600	FG FG F G FG F G G FF	7 1 3	2 1/2 3/4 5/8	1 1 5/8
25	255 Mo 58 MnO	1400 1500 1600	FG FG F G G FF G G FF	3 4 2	2 2 3/4	3/4 0 5/8
26	210 Mo 116 MnO	1400 1500 1600	G F FF G G G F F F	3/4 3/4 1/2	0 3/4 3/4	0 0 1/4
27	210 Mo 90 Fe	1250 1300 1350	FG F G G FG FG F FG	2	3/4 3/4 7/8 2 1/2 3/4	1/2 3/4 3/4
28	255 Mo 45 Fe	1250 1300 1350	FF FF FF FG FG P FF FF FF	1/2 1/2 3/4	0 1/2 1/4	0 1/4 3/4
29	210 Mo 129 Fe_2O_3	1250 1300 1350	P P P P P P P P P	0 0 1/4	0 1/4 0	0 0 0

*P-poor, F-fair, G-good

**Torque in inch-pounds

TABLE 2 (Cont.)

RESULTS OF ADHERENCE TESTS AND TORQUE PEEL TESTS PERFORMED ON SPECIMENS METALLIZED WITH COMPOSITIONS BASED ON THE ALUMINA REACTION THEORY

Composition Number	Composition and Weight (gr)	Sintering Temp (°C)	Adherence Rating* AD-94	AD-96	AL-23	Torque Peel Value** AD-94	AD-96	AL-23
30	25% Mo 64% Fe_2O_3	1250 1300 1350	FF F PF F FF FF PF FF PF			0 1/2 1/2	0 1/2 1/2	0 1/2 1/4
31	210 Mo 90 Ti	1500 1600 1700	G F FF F G FG G G FF			2 1 1/2 4	1 1 1/2 2	1 1 1/2 2
32	25% Mo 45 Ti	1500 1600 1700	G G FF G G FG G G FF			2 4 2	1 2 3/4 1 3/4	3/4 3/4 3/4
33	210 Mo 150 TiO_2	1500 1600 1700	G FG FF G G F G G FF			1 3/4 1 1/2 2	3/4 1 3/4 2	3/4 3/4
34	25% Mo 75 TiO_2	1500 1600 1700	G G FF G FG FG G G F			3/4 2 1/2 4	3/4 1 1/4 2	1/2 1/2 2
35	210 Mo 50 BaO 96.5 SiO_2	1400 1500 1600	G G G F F G FG F FG			3/4 3/4 3/4	3/4 1 3/4	2 1/2 2 2 1/2
36	25% Mo 25 BaO 40 SiO_2	1400 1500 1600	FF G FG F F G FG F FG			1 1/2 3/4 3/4	3/4 1 1 1/4	1 1/2 2 3/4
37	210 Mo 63 CaO 64 Fe_2O_3	1300 1400 1500	F F F FF FF FF F F F			1/2 3/4 1	3/4 3/4 1	3/8 0 1
38	25% Mo 31 CaO 32 Fe_2O_3	1300 1400 1500	F F F FG FG FG F F F			1/2 4 1	3/4 2 3/4	3/4 0 1
39	210 Mo 45 Fe 96.5 SiO_2	1300 1400 1500	FF FF FF F G G F F G			1/4 3/4 1 1/4	3/4 3/4 1	3/4 0 1 1/2
40	25% Mo 22 Fe 40 SiO_2	1300 1400 1500	FF FF F FF F G G G			1/2 0 3/4	1/2 3/4 3/4	1/4 1 7/8
41	210 Mo 64 Fe_2O_3 96.5 SiO_2	1300 1400 1500	F FF F FG G F F F G			1/2 0 1/2	1/2 5/8 3/4	1/2 1 1/2 3/4
42	25% Mo 32 Fe_2O_3 40 SiO_2	1300 1400 1500	F FF F FG G F G G G			1/2 3/4 3/4	1/2 5/8 3/4	1/2 3/4 7/8
43	210 Mo 90 Feldspar	1400 1500 1600	FF F G G G G G FG G			1 1/2 3/4 2 1/2	2 3/4 3/4	1 1/2 3 1 1/2
44	25% Mo 45 Feldspar	1400 1500 1600	FF F FG G F FG G G G			3/4 7/8 3 1/2	1/2 1/2 2 1/2	2 1/4 1 3/4 2 1/2
45	210 Mo 30 Talc	1400 1500 1600	F FF FG F FF G G FG G			1/2 7/8 3/4	3/4 5/8 1/2	2 3/4 1 1/2
46	25% Mo 45 Talc	1400 1500 1600	FG FF F G FF F G G G			3/4 3/4 4	0 3/4 2 1/2	3/4 0 3
47	96.5 SiO_2 5% MnO 210 Mo	1300 1400 1500	G GE GE FG FG F G F F			1/2 1 3/4	1/2 1 1/2 3/4	1 1/2 3/4 3/4
48	210 Mo 96.5 SiO_2 4% Mn	1300 1400 1500	G GE GE FG FG FG G G FF			1 1/2 3/4 3/4	1/2 3/4 1/2	1/4 3/4 3/4
49	25% Mo 40 SiO_2 2% MnO	1300 1400 1500	G G G FG FG FG G G G			1 1/2 1 1/4 1 1/8	1/2 3 1	1/4 1 1/2 2 3/4
50	25% Mo 40 SiO_2 22 Mn	1300 1400 1500	G G G FG FG FG G FF G			2 2 3/4	2 3 3/4	1 1 2
51	210 Mo 96.5 SiO_2 5% ZnO	1500 1600 1700	F F G FG FG FG G FF FF			3/4 3/4 1	7/8 1/2 1/2	2 3/4 3/4
52	210 Mo 96.5 SiO_2 4% Zr	1500 1600 1700	F F G FG FG FG G FF FF			3/4 3/4 1	1/2 3/4 1/2	0 3/4 1/4
53	25% Mo 40 SiO_2 20 ZnO	1500 1600 1700	FF F G G FG G G G FF			2 2 4	3/4 7/8 1 1/4	7/8 3 1/2 1/2
54	25% Mo 40 SiO_2 22 Zn	1500 1600 1700	FF F F G FG G G G FF			3/4 1 1/2 2	3/4 3/4 1	7/8 2 1/2
103	270 Mo 30 Talc	1400 1500 1600	FF FF FF F FF FF G G G			1/2 3/4 5	3/4 3/4 2 1/2	1 5/8 1 1/2

*P-poor, F-fair, G-good

**Torque in inch-pounds

TABLE 2 (Cont.)

RESULTS OF ADHERENCE TESTS AND TORQUE PEEL TESTS PERFORMED ON SPECIMENS METALLIZED WITH COMPOSITIONS BASED ON THE ALUMINA REACTION THEORY

Composition Number	Composition and Weight (gr)	Sintering Temp (°C)	Adherence Rating* AD-94	AD-96	AL-23	Torque Peel Value** AD-94	AD-96	AL-23
104	85 Mo 15 TaN	1400	FF	FF	FF	3/4	7/8	3/4
		1500	G	F	F	3/4	3/4	3/4
		1600	G	G	F	4 1/2	2	3/4
130	40 Mo 51 Mn 12 ZrO_2	1400	FG	F	F	2 1/2	7/8	3/4
		1500	G	G	FF	1 1/2	3/4	3/4
		1600	G	G	FF	3	1 1/2	3/4
136	40 Mo 37 Mn 41 ZrO_2	1400	G	FG	FG	1 1/2	3/4	3/4
		1500	G	G	F	1 1/4	1	3/4
		1600	G	G	F	2	3	1
146	50 Mo 50 Mn	1400	G	G	G	1 1/4	3/4	1 1/4
		1500	F	F	G	3/4	1/2	1/2
		1600	G	FG	FG	1 1/2	1	1/2
147	80 Mo 60 Mn 60 Fe	1300	FG	F	F	3/4	1/2	1/2
		1400	G	G	G	3/4	3/4	3/4
		1500	FF	F	F	1/2	5/8	1/2
148	40 Mo 30 Mn 30 Fe	1300	FG	F	F	1	3/4	1/2
		1400	G	FG	FG	2 1/2	1	1/2
		1500	F	FF	FF	5/8	1/4	1/2
149	40 Mo 45 Mn 15 Fe	1300	FG	F	F	2	3/4	3/4
		1400	G	FG	FG	3/4	3/4	1/2
		1500	G	FF	FF	3/4	1/4	1/2
150	80 Mo 105 Mn 15 Fe	1300	G	FG	FG	2	3/4	0
		1400	G	FG	FG	3/4	3/4	3/4
		1500	G	F	F	1/2	1/4	5/8
151	180 Mo 15 Mn 105 Fe	1300	FG	F	F	1/2	1/2	1/2
		1400	G	G	G	1/2	3/8	3/4
		1500	FG	F	F	1/2	7/8	3/4
152	240 Mo 15 Mn 45 Fe	1300	FG	F	FF	5/8	3/4	1/2
		1400	GVG	G	G	1	1/2	3/4
		1500	FF	FF	F	1/2	7/8	5/8
161	240 W 60 Mn	1400	G	G	FG	1/2	1/2	1
		1500	G	G	FF	1/2	3/8	1/2
		1600	F	F	FF	3/4	3/4	1
163	240 W 30 Mn 30 Fe	1300	FF	FF	FF	1/4	1/4	1/4
		1400	FF	FF	FF	1/4	1/2	0
		1500	F	FF	F	1/2	1/2	1/2
165	240 W 60 Fe	1250	F	F	F	0	1/2	1/2
		1300	FF	FF	F	1/2	0	0
		1350	FF	FF	FF	3/4	0	1/4
		1500	F	F	F	1/2	1/2	1/2
200	240 Mo 60 Mn	1400						
		1500	G	FG	F			
		1600						

*P-poor, F-fair, G-good

**Torque in inch-pounds

TABLE 3

RESULTS OF ADHERENCE TESTS AND TORQUE PEEL TESTS PERFORMED ON SPECIMENS METALLIZED WITH COMPOSITIONS BASED ON THE MOLYBDENUM OXIDE THEORY

Composition Number	Composition and Weight (gr)	Sintering Temp. (°C)	Adherence Rating*			Torque Peel Values**			Composition Number	Composition and Weight (gr)	Sintering Temp. (°C)	Adherence Rating*			Torque Peel Values**		
			AD-94	AD-96	AL-23	AD-94	AD-96	AL-23				AD-94	AD-96	AL-23	AD-94	AD-96	AL-23
55	150 Mo 91 MoO_3 100 BaC	1500 1600 1700	P P P G FG FF F FF FF			3/4 3/4 3/4	1/2 3/4 1/2	0 3/4 0	61	150 Mo 91 MoO_3 112 ZnO	1500 1600 1700	G F F G G F G F FF			3/4 3/4 1/2	3/4 1 1/4 3/4	1/2 1 1/4 1/2
56	150 Mo 91 MoO_3 126 CaO	1300 1400 1500	P P FF FG FG FG G G G			3/4 1 1/2 1 1/2	3/4 1 1/2 1 3/4	3/4 3/4 1 1/2	62	150 Mo 91 MnO_3 121 ZrO_2	1500 1600 1700	G G P G G FF G F FF			1 1/2 1 1/4 3/4	1 1 3/4 3/4	3/4 1/4 1/2
57	150 Mo 91 MoO_3 150 MgO	1500 1600 1700	G G P G FG F F FF FF			7/8 2 1/2	0 3/4 1/4	0 5/8 0	63	150 Mo 91 NiO_4 142 MnO_2	1400 1500 1600	F F F G G F G FG FF			1 1 1/4 1	1 1/2 1	3/4 3/4 3/4
58	150 Mo 91 MoO_3 193 SiO_2	1400 1500 1600	FF F FF F F G G F G			0 3/4 1/4	1/2 0 3/8	3/4 1 1 1/4	64	150 Mo 91 MnO_4 129 Fe_2O_3	1250 1300 1350 1500	F FF FF FF F FF FF FF FF G F F			1/2 1/2 1/2 3/4	0 0 0 1/4	5/8 5/8 1/4 3/4
59	150 Mo 91 MoO_3 123 SrO	1500 1600 1700	FF F F FF FF F FF FF FF			3/4 0 1/2	1/2 0 0	0 0 0	178	150 Mo 90 MnO_3 60 MnO_2	1400 1500 1600	G FG FG G FG FF G FG FF			2 1 1	1/2 1 1/4 1 1/2	1/2 1/2 3/4
60	150 Mo 91 MoO_3 102.5 TiO_2	1500 1600 1700	F FG F G FG FF G F F			3/4 1 1/4 1 1/2	3/4 3/4 1/2	0 1/4 1/4	199	300 MnO_3	1300 1400 1500 1600 1700	F F F F FF F F F F G G FF G G F			2 1/2 3/4 2 1/2 1 1	1 3/4 3 1 1/2 1 1/4	1 3/4 3/4 3/4 1/2

*P-poor, F-fair, G-good
**Torque in inch-pounds

TABLE 4

MATERIALS WHICH LOWER GLASS VISCOSITY

Material	Source	Material	Source
TiO_2	TiO_2	Li_2MnO_3	Li_2MnO_3
CeO_2	CeO_2	Li_2TiO_3	Li_2TiO_3
Na_2O	Na_2O_2	$MgO \cdot SiO_2$	Talc
K_2O	Potassium Carbonate	$K_2O \cdot Al_2O_3 \cdot 6SiO_2$	Feldspar
BaO	BaO	Rb*	
B_2O_3	Boric Acid	Cs*	
Li_2O	Lithium Carbonate		

*Prices prohibitively high

TABLE 5

RESULTS OF ADHERENCE TESTS AND TORQUE PEEL TESTS PERFORMED ON SPECIMENS METALLIZED WITH COMPOSITIONS BASED ON THE GLASS MIGRATION THEORY

Composition Number	Composition and Weight (gr)	Sintering Temp. (°C)	Adherence Rating* AD-94	AD-96	AL-23	Torque Peel Value** AD-94	AD-96	AL-23
65	292.5 Mo 7.5 Ti	1500 1600 1700	G G P G G F G G FG	2 1/2 4 4	1 1/2 3 6	1/2 1 1
66	285 Mo 15 Ti	1500 1600 1700	G G FP G G F G G F	1 3 1/2 6	1 1/4 2 9	3/4 1 3/4
67	270 Mo 30 Ti	1500 1600 1700	G G F G G G G G FF	2 3 4	3/4 2 5	3/4 3/4 1
68	292.5 Mo 9.2 CaO_2	1500 1600 1700	FG G FP G G FF G G FF	2 2 1/2 7	1/2 6 4	1/2 3/4 1/4
69	285 Mo 18.4 CaO_2	1500 1600 1700	G G F G G F G G FF	1 2 5	3/4 4 4	3/4 3/4 1/2
70	270 Mo 36.8 CaO_2	1500 1600 1700	G F FP FG G F G G G	1 1/2 2 4	3/4 2 1/2 1/2	3/4 1 1
71	240 Mo 60 Ti	1500 1600 1700	G F FP G G G G F F	1 1 6	1/2 3/4 1/2	1 1/2 1 3/4
72	240 Mo 73.6 CaO_2	1500 1600 1700	G G FP G G FF G F FF	2 2 4	2 2 3/4	3/4 1/2 1 1/4
73	292.5 Mo 17.3 Na_2CO_3	1500 1600 1700	FG F F G FG FF G F FF	1/2 2 5	3/4 3/4 3/4	1/2 5/8 3/4
74	296 Mo 8.6 Na_2CO_3	1500 1600 1700	F F F G FG FF G FG FF	3/4 4 1 1/4	3/4 1 1/2 3/4	1/2 1/4 1/4
75	285 Mo 34.6 Na_2CO_3	1500 1600 1700	FG F P G FG FF G F FF	1 3 3 1/2	1/2 1 3/4	7/8 1/4 0
76	270 Mo 69.2 Na_2CO_3	1500 1600 1700	G G P G FG P G F FF	3/4 3/4 1	1 5/8 1	5/8 1/2 3/4
77	292.5 Mo 13.3 K_2CO_3	1500 1600 1700	G F P G FG P G G F	3/4 3/4 2	3/4 1/2 3/4	0 1/4 1/4
78	296 Mo 6.7 K_2CO_3	1500 1600 1700	G F P G FG P G G FF	1 3/4 3	3/4 1 1/4 7 1/4	5/8 1/4 0
79	285 Mo 26.6 K_2CO_3	1500 1600 1700	F FF F G FG P G FG FF	3/4 1 1/4 4	3/4 1/2 1	7/8 1/4 0
80	270 Mo 53.2 K_2CO_3	1500 1600 1700	FG G P FG P P G FG F	1 1/2 3/4 1 1/2	3/4 1/2 3/4	3/4 0 0
81	292.5 Mo 5.4 BaO	1500 1600 1700	G G P G FG P G FG F	3/4 3 2	1 1/2 3/4 1	1/2 1/4 1/4
82	285 Mo 16.8 BaO	1500 1600 1700	FF P P FG F FF G FG F	3/4 2 1 1/4	1/2 1/2 1	3/4 1/4 1/4
83	270 Mo 33.6 BaO	1500 1600 1700	FF P P G F FF G F FG	5/8 1 1/4 3/4	1/2 1/2 1	1/2 1/4 1/4
84	240 Mo 67.2 BaO	1500 1600 1700	FF P P G F F G F F	1/2 3/4 3/4	1/2 1/2 1	3/4 1/4 1/2
85	292.5 Mo 43 H_3BO_3	1500 1600 1700	F FG FF FG F FF G F F	1/2 1 1	1/2 5 1	1/4 1/2 0
86	296 Mo 21 H_3BO_3	1500 1600 1700	F F F G F FF G FG FF	1/2 3 1/2 3	1/2 3/4 3/4	3/4 1/4 1/4
87	285 Mo 86 H_3BO_3	1500 1600 1700	F FG P FG FF FF G F FF	1/2 1 2	1/2 1/4 3/4	1/2 1/4 1/2
88	246 Mo 3.75 Lithium Manganate	1300 1400 1500	G F F F F FF G G F	3 1 3/4 7/8	3/4 1/2 7/8	1/2 0 5/8
89	292.5 Mo 7.5 Lithium Manganate	1300 1400 1500	G F F FF FF FF G G FF	3/4 0 3/4	3 3/4 5/8	1 1/4 1/2 1/2
90	285 Mo 15 Lithium Manganate	1300 1400 1500	G F F FG F F G G FF	1/2 1 3/4 1	3/4 5/8 3/4	1/4 3/4 3/4

*F-poor, F-fair, G-good

**Torque in inch-pounds

TABLE 5 (Cont.)

RESULTS OF ADHERENCE TESTS AND TORQUE PEEL TESTS PERFORMED ON SPECIMENS METALLIZED WITH COMPOSITIONS BASED ON THE GLASS MIGRATION THEORY

Composition Number	Composition and Weight (gr)	Sintering Temp (°C)	Adherence Rating* AD-94	AD-96	AL-23	Torque Peel Value** AD-94	AD-96	AL-23
91	270 Mo 30 Lithium Manganate	1300	F	F	F	3/8	1/2	1/2
		1400	FG	F	F	1 1/4	3/4	3/4
		1500	FG	FG	FF	2	5/8	5/8
92	240 Mo 60 Lithium Manganate	1300	F	F	F	3/4	3/4	3/4
		1400	FG	F	FF	3/4	5/8	3/4
		1500	G	G	FF	7/8	5/8	3/4
93	296 Mo 3.75 Lithium Titanate	1300	F	F	F	5/8	3/4	3/4
		1400	FG	F	F	1	3/4	5/8
		1500	G	FG	G	1	3/4	3/4
94	292.5 Mo 7.5 Lithium Titanate	1300	F	F	F	1 1/4	1	1/4
		1400	FG	F	F	3	1 3/4	3/4
		500	G	FF	FF	3/4	1/2	3/4
95	285 Mo 15 Lithium Titanate	1300	F	F	F	2	3/4	1/4
		1400	FG	F	F	1 1/2	1	3/4
		1500	F	FF	FF	1/2	1/2	7/8
96	270 Mo 30 Lithium Titanate	1300	F	F	F	3/4	1	3/4
		1400	FG	FG	FG	3	3	3/4
		1500	G	F	FG	3/4	1/2	3/4
97	240 Mo 60 Lithium Titanate	1300	F	F	F	3/4	1/2	1/2
		1400	FG	FG	FG	1	3/4	3/4
		1500	G	F	F	2 1/2	3/4	1
98	296 Mo 3.75 Lithium Carbonate	1300	F	F	FF	0	0	0
		1400	F	F	FF	1	0	0
		1500	G	F	F	3/4	3/4	1/8
99	292.5 Mo 7.5 Lithium Carbonate	1300	FG	F	F	3/4	0	0
		1400	F	FF	F	3	1/4	1/4
		1500	F	F	F	1/4	3/4	1/2
100	285 Mo 15 Lithium Carbonate	1300	F	F	FF	3/4	1/2	0
		1400	F	F	F	1 1/2	0	0
		1500	F	F	FF	3/4	3/4	3/4
101	270 Mo 30 Lithium Carbonate	1300	F	F	FF	1/2	1/2	0
		1400	F	F	FF	3/4	0	0
		1500	F	FF	FF	3/4	3/4	3/4
102	240 Mo 60 Lithium Carbonate	1300	F	F	FF	1/2	3/4	0
		1400	FF	FF	FF	1/4	0	0
		1500	FF	FF	FF	3/4	3/4	3/4

*F-poor, F-fair, G-good

**Torque in inch-pounds

TABLE 6

RESULTS OF ADHERENCE TESTS AND TORQUE PEEL TESTS PERFORMED ON SPECIMENS METALLIZED WITH COMPOSITIONS BASED ON THE MOLYBDENUM SINTERING THEORY

Composition Number	Composition and Weight (gr)	Sintering Temp. (°F)	Adherence Rating* AD-94	AD-96	AL-23	Torque Peel Value** AD-94	AD-96	AL-23
107	300 Mo	1250	FF	FF	P	0	0	0
		1300	FF	FF	FF	3/4	1/2	0
		1350	FF	FF	FF	3/4	1/4	1/4
		1400	FF	FF	FF	1 1/2	5/8	1/4
		1500	G	G	P	7/8	5/8	0
		1600	G	FG	FF	4	1 1/2	1/4
108	300 Mo	1500	G	F	P	3/4		0
		1600	G	FG	FF	4 1/2	1	1/4
	0.9 Fe	1700	G	G	FG	5	3	1/4
109	297 Mo	1500	G	FF	P	7/8	7/8	0
		1600	G	FG	FF	4 1/2	2 1/2	1/4
	3 Fe	1700	G	FG	FF	4	4	1/4
110	291 Mo	1500	G	F	P	5/8	1/2	1/2
		1600	G	F	FF	4	1 1/2	1/4
	9 Fe	1700	G	FG	F	3 1/2	2	1/4
111	270 Mo	1500	G	F	P	3/4	1/2	1/4
		1600	G	F	FF	7	3/4	1/4
	30 Fe	1700	G	FG	FF	1 1/4	1	1/4
112	300 Mo	1500	G	F	P	7/8	3/4	1/4
		1600	G	FG	FF	3 1/2	3 1/2	1/4
	0.9 Ni	1700	G	FG	FF	10	1	0
113	297 Mo	1500	G	FF	P	1/2	1/2	0
		1600	G	FF	FF	1	1/4	1/4
	3 Ni	1700	G	F	FF	1	0	0
114	291 Mo	1500	G	F	P	1/2	1/2	-
		1600	FG	FF	P	1	1/4	1/4
	9 Ni	1700	G	FF	P	3/4	1/2	0
115	270 Mo	1500	P	P	P	1/2	1/2	1/4
		1600	FG	FF	FF	3/4	1/2	1/4
	30 Ni	1700	P	FF	P	5/8	1/4	0
116	300 Mo	1500	G	F	P	3/4	3/4	1/4
		1600	G	G	FF	5	4	1/2
	0.9 Co	1700	G	G	FF	5	5	0
117	297 Mo	1500	G	F	P	1/2	1/2	1/2
		1600	G	FG	FF	3	3	1/2
	3 Co	1700	G	FG	FF	4	3/4	1/4
118	291 Mo	1500	F	P	P	1/2	1/2	7/8
		1600	G	FF	FF	5	1/2	1/4
	9 Co	1700	FG	F	FF	1 1/4	3/4	1/4
119	270 Mo	1500	G	G	P	1/2	5/8	3/4
		1600	G	FF	FF	1/2	3/4	1/4
	30 Co	1700	F	FF	FF	3/4	1/4	1/4
120	300 Mo	1500	G	FG	P	3/4	5/8	3/4
		1600	G	FF	FF	4 1/2	1 1/2	1/4
	0.9 W	1700	G	FF	FF	4	1	1/2
121	297 Mo	1500	FG	F	P	1	3/4	1/2
		1600	G	FG	FF	5 1/2	4 1/4	1/2
	3 W	1700	G	F	FF	7	1	0
122	291 Mo	1500	FG	FF	P	3/4	5/8	3/4
		1600	G	FG	FF	8	2	1/2
	9 W	1700	G	FF	FF	3	3/4	0
123	270 Mo	1500	FG	FF	P	3/4	5/8	3/4
		1600	G	G	FF	4	2 1/2	1/2
	30 W	1700	G	FF	FF	7	3/4	3/4

*P-poor, F-fair, G-good

**Torque in inch-pounds

TABLE 7

RESULTS OF ADHERENCE TESTS AND TORQUE PEEL TESTS PERFORMED ON SPECIMENS METALLIZED WITH COMPOSITIONS BASED ON THE GLASS ADDITIVE THEORY

Composition Number	Composition and Weight (gr)	Sintering Temp. (°C)	Adherence Rating* Ab-96	Ab-96	Al-23	Torque Peel Value** Ab-96	Ab-96	Al-23
105	270 Mo 30 Feldsper	1400 1500 1600	F FF FF G G G G G F			1/2 3/4 4	3/4 3/4 2	7/8 5/8 2
106	285 Mo 15 Feldsper	1400 1500 1600	F FF FF G F F G FG F			7/8 3/4 3	1/4 5/8 3	3/4 1/2 5/8
124	240 Mo 24 Mn 15 Fe 9 SiO_2 9 CaO	1300 1400 1500	FG FG F FF F FF F F FF			3/4 1 3/4	3/4 7/8 3/4	3 5/8 1/2
125	200 Mo 40 Mn 10 Fe 2 SiO_2 2 CaO	1300 1400 1500	FG F F FG FG FF G F F			3/4 1 3/4	3/4 3/4 3/4	3/4 3/4 1/2
141	291 Mo 9 Talc	1500 1600 1700	G G FF G G FF G F FF			7/8 4 5	3/4 3 1/2 1 1/4	5/8 1/2 1
154	240 Mo 30 $Al(OH)_3$ 10 Ben-tonite 20 Kaolin	1300 1400 1500	FF FF FF FG F F FF F F			0 1/2 3/4	0 1/4 1/2	0 3/4 0
155	291 Mo 9 Alumino Silicate Glass	1300 1400 1500	FG FF FF FG F F FG FG FF			1/2 1 1/4 5/8	0 3/8 1/2	1/2 3/4 1/2
156	270 Mo 30 Corning 1723 Glass	1300 1400 1500	FF FF FF FG F FG F G F			1/2 1 1/4 3/4	1/4 3/4 1/2	1/2 3/4 1/2
134	285 Mo 15 V_2O_5	1300 1500 1700	F FF FF FG FG F G G FF			3/4 1 1/8 7	0 3/4 7	1/2 1/2 1/2
135	285 Mo 15 P	1300 1400 1500	F FF FF F FF FF FG FG F			1/4 1 3/4	0 0 1/2	0 0 1/4
130	285 Mo 15 As_2O_3	1300 1400 1500	F FF FF F FF F FF FF F			3/4 5/8 5/8	1/2 0 1/8	0 0 0
137	285 Mo 15 SiO_2	1400 1500 1600	FF F FF F FF F G G F			1 3/8 5/8 6	1/2 1/2 5	1/2 1/2 3

*P-poor, F-fair, G-good

**Torque in inch-pounds

TABLE 8

RESULTS OF ADHERENCE TESTS AND TORQUE PEEL TESTS PERFORMED ON SUBSTRATES METALLIZED WITH OTHER COMPOSITIONS

Composition Number	Composition and Weight (gr)	Sintering Temp. (°C)	Adherence Rating* AD-94	AD-96	AL-23	Torque Peel Values** AD-94	AD-96	AL-23
126	270 W	1300	FF	FF	F	1/4	0	0
		1500	F	F	F	0	0	1/2
	30 Fe	1700	F	FF	F	3/4	0	0
127	240 Mo	1300	F	F	FF	1/2	3/4	1/4
	30 Mn							
	30 Co	1400	FG	F	FF	1/4	3/4	3/4
		1500	G	F	FF	3/4	7/8	1/2
128	240 Mo	1400	FG	F	F	3 1/2	5/8	1/2
	51 Mn	1500	G	F	FF	1/2	3/4	1/2
	9 Zn	1600	G	F	FF	3 1/2	1	1/2
129	240 Mo	1400	G	FG	FG	3	1	3/4
	51 Mn	1500	G	G	F	7/8	5/8	3/4
	9 Ti	1600	G	G	F	3 1/2	1	1/2
131	240 Mo	1400	FG	FG	F	2 1/2	2	3/4
	42 Mn							
	9 Ti	1500	G	G	FG	1/2	5/8	5/8
	12 ZrO_2	1600	G	G	F	3	1 1/2	1/2
132	240 Mo	1500	G	G	FG	1/2	7/8	5/8
		1600	G	G	FG	3 1/2	1 1/2	1
	66 TiC	1700	G	FG	F	6 1/2	3/4	
133	240 Mo	1400	F	FF	FF	3/4	1/2	1/2
	30 Mn	1500	FF	FF	F	5/8	5/8	1/4
	35.5 SrO	1600	F	F	FF	3/4	3/4	1/4
134	240 Mo	1400	FG	FG	F	1 1/2	1	7/8
	30 Mn	1500	FG	F	F	5/8	5/8	5/8
	30 Zn	1600	G	G	F	4 1/2	2 1/2	3/4
135	240 Mo	1400	FG	FG	FG	2 1/2	2	3/4
	30 Mn	1500	G	G	G	5/8	1 1/2	1/4
	30 Ti	1600	G	G	FG	3 1/2	3	5/8
137	210 Mo	1400	G	FG	F	2	1 1/2	3/4
	30 Mn							
	30 Ti	1500	G	G	G	3	3	7/8
	41 ZrO_2	1600	G	G	G	2 1/2	2 1/2	1 1/4
138	240 Mo	1400	G	FG	FG	3 1/2	3 1/2	3/4
	30 Mn	1500	G	G	G	2 1/4	7/8	7/8
	30 TiC	1600	G	G	G	4 1/2	4	3/4
139	240 Mo	1250	F	F	F	5/8	3/4	1
	36 O'Hommel Sealing Glass #5000	1300						
		1350	FF	FF	F	3/4	3/4	3/4
		1500	FG	F	F	3/4	5/8	5/8
	19.2 Co							
	4.8 Sn							
140	240 Mo	1400	G	FG	F	3	3/4	1
	51 Mn	1500	G	G	FF	1 1/4	5/8	1/2
	9 Talc	1600	G	G	F	4	3 1/2	1 1/4
142	276 Mo	1400	FG	FG	F	2	3/4	3/4
	15 Fe	1500	FG	F	FF	5/8	3/4	1/2
	9 Talc	1600	G	FG	FF	4 1/2	2	1/2
143	279 Mo	1400	FG	FG	F	2 1/2	3/4	1/2
	15 Fe							
	2 Kaolin	1500	FG	F	FF	5/8	3/4	1/2
	4 Talc	1600	G	F	FF	5 1/2	1 1/2	1/2
144	279 Mo	1400	G	FG	F	2	3/4	3/4
	15 Mn							
	2 Bento-nite	1500	G	F	FF	3/4	5/8	1/2
	4 Kaolin	1600	G	G	F	4 1/2	4 1/2	1/4
145	240 Mo	1400	G	G	G	2 1/2	1/2	3/4
	51 Mn							
	6 Bento-nite	1500	G	G	FF	3/4	5/8	1/2
	3 Kaolin	1600	G	G	F	5	3	3/4
153	225 Mo	1400	G	G	G	2 1/2	1/2	5/8
	50 Mn	1500	G	G	FF	1/2	5/8	5/8
	15 $Al(OH)_3$	1600	G	G	FF	3 1/2	2 1/2	3/4
157	200 MnO_2	1250	FF	FF	FF	1/2	0	1/4
	100 CoO^2	1300	FG	F	F	1/4	0	1/4
	100 Fe_2O_3	1350	F	FG	FF	3/4	1/2	1/4
		1500	F	F	F	0	0	0
158	100 MnO_2	1250	FF	FF	F	3/4	0	5/8
	50 CoO^2	1300	FF	FF	FF	1/4	1/2	1/4
	150 Fe_2O_3	1350	F	FG	FG	3/4	3/4	0
		1500	F	F	F	0	0	0
159	100 MnO_2	1250	FF	F	FF	1/2	0	0
	150 CoO^2	1300	FG	F	FF	1/4	1/4	1/4
	50 Fe_2O_3	1350	F	F	FG	3/4	1/4	1/4
		1500	F	F	F	0	0	0
160	120 MoO_3	1400	G	G	FG	1/2	1/2	1/4
	120 WO_3	1500	G	G	FF	5/8	1/2	1/4
	60 Mn	1600	G	G	G	1 1/2	1	3/4
162	240 MoO_3	1400	G	G	FG	1/2	5/8	1/2
		1500	FG	F	FF	1/2	1/2	1/2
	60 Mn	1600	F	F	FF	1 1/2	1	1/2
164	240 MoO_3	1400	FG	G	G	1 1/2	1 1/2	1/4
		1500	G	G	G	5/8	1/2	5/8
	60 MnO_2	1600	G	G	F	2	4	1/2

*F-poor, V-fair, G-good

**Torque in inch-pounds

TABLE 6 (Cont.)

RESULTS OF ADHERENCE TESTS AND TORQUE PEEL TESTS PERFORMED ON SPECIMENS METALLIZED WITH OTHER COMPOSITIONS

Composition Number	Composition and Weight (gr)	Sintering Temp. (°C)	Adherence Rating* AD-94	AD-96	AL-23	Torque Peel Value** AD-94	AD-96	AL-23
166	240 WO_3	1400	FG	FG	G	1/4	3/4	1/2
		1500	G	G	G	1 1/2	1 1/4	3/4
	60 Mo	1600	G	FG	P	1	3/4	0
167	240 W 51 Mn 3 Bento-nite 4 Kaolin	1400	FP	FP	FP	3/4	3/4	1/2
		1500	FP	FP	P	3/4	3/4	3/4
		1600	FP	FP	P	3/4	3/4	3/4
168	240 WO_3	1400	G	FG	P	3/4	3/4	0
		1500	G	G	G	1/2	1 1/2	3/4
	60 MnO_2	1600	G	G	G	1	3/4	1/2
169	120 $LiMoO_4$ 120 K_2MoO_4 60 Mn	1300	P	P	FP	1	1	3/4
		1400	G	FG	G	1	1/2	3/4
		1500	G	G	G	3/4	5/8	3/4
170	60 Mo 222 Fe 3 Cu 15 Mn	1300	P	P	FP	1/4	3/4	1/4
		1400	FP	FP	FP	3/4	3/4	1/2
		1500	FP	P	P	1/2	1/2	3/4
171	60 Mo 222 Fe 3 Cu 15 Co	1300	FP	FP	FP	1/4	1/4	0
		1400	P	FP	FP	1/4	3/8	1/4
		1500	P	P	P	1/2	5/8	5/8
172	60 Mo 222 Fe 3 Cu 21 CaO	1300	FP	FP	FP	1/4	3/4	1/2
		1400	P	FP	P	1/2	1/4	0
		1500	P	P	P	0	1/2	0
173	60 Mo 222 Fe 3 Cu 15 Si	1300	P	FP	P	1/4	1/4	3/4
		1400	FG	P	G	1/4	3/4	1/2
		1500	P	P	P	1/2	1/2	1/2
174	60 Mo 222 Fe 3 Cu 20 ZrO_2	1300	FP	FP	FP	1/4	1/4	0
		1400	G	G	P	1/2	1/2	1/4
		1500	P	P	P	3/4	1/2	1/2
175	295 Mo 30 Mn 15 Li_2CO_3	1400	G	G	P	3/4	1/2	1/4
		1500	G	FG	P	1 1/4	3/4	7/8
		1600	G	G	FP	2	3 1/2	1/4
176	195 Mo 90 Mn 15 Li_2CO_3	1400	G	G	FG	1 1/4	3/4	1/2
		1500	FG	FG	P	1	5/8	7/8
		1600	G	G	P	2	3/4	1/2
177	135 Mo 150 Mn 15 Li_2CO_3	1400	G	G	FG	1	3/4	1/2
		1500	G	G	FG	1	3/4	7/8
		1600	FG	P	P	2	1	1
179	165 Zircon 30 ZrO_2 66 Talc 12 Kaolin 18 Ba_2CO_3 21 O'Hommel Sealing Glass #5000	1300	G	G	G	1/4	1/4	1/4
		1400	G	G	G	3/4	3/4	1/4
		1500	P	P	P	0	0	0
180	240 Corning 7052 45 Fe_2O_3 15 Mo	1300	G	G	G	1/4	1/4	1/4
		1400	G	G	G	1/2	1/4	1/4
		1500	P	P	P	0	0	0
181	240 Cr 60 O'Hommel Sealing Glass #5000	1400	FG	FG	FG	1/2	1/4	1/4
		1500	FP	P	P	1/2	1/4	1/2
		1600	G	P	P	0	0	0
182	240 Si 60 O'Hommel Sealing Glass #5000	1250	G	G	G	0	0	1/2
		1300	G	G	G	1/4	0	1/2
		1350	G	G	G	0	0	0
		1500	P	P	G	5/8	1/2	1/2
183	120 Al_2O_3 120 O'Hommel Sealing Glass #5000 60 Fe	1300	G	G	G	0	0	1/4
		1400	FG	G	FG	3/4	5/8	5/8
		1500	G	G	G	5/8	1/2	5/8
184	60 Al_2O_3 60 O'Hommel Sealing Glass #5000	1300	FG	FG	FG	1/2	0	1/2
		1400	P	FG	FG	3/4	5/8	5/8
		1500	P	P	P	3/4	3/4	1
185	120 Al_2O_3 120 O'Hommel Sealing Glass #5000 60 Cu	1300	G	G	G	0	0	0
		1400	G	G	G	0	0	0
		1500	G	G	G	3/4	5/8	5/8

*P-poor, F-fair, G-good

**Torque in inch-pounds

TABLE 8 (Cont.)

RESULTS OF ADHERENCE TESTS AND TORQUE PEEL TESTS PERFORMED ON SPECIMENS METALLIZED WITH OTHER COMPOSITIONS

Composition Number	Composition and Weight (gr)	Sintering Temp. (°C)	Adherence Rating* AD-94	AD-96	AL-23	Torque Peel Value** AD-94	AD-96	AL-23
186	90 Al_2O_3 90 O'Hommel Sealing Glass #5000 120 Mo	1300	G	G	G	1/4	1/4	1/4
		1500	G	G	G	1 5/8	1 5/8	3/4
		1700	G	G	G	2	3	1 1/2
187	30 Al_2O_3 30 O'Hommel Sealing Glass #5000 240 Mo	1300	F	F	FG	3/4	1/2	3/4
		1500	G	FG	G	3/4	7/8	3/4
		1700	FG	F	FF	2	1	3/4
188	180 Feldspar 120 Ni	1300	FG	FG	G	1/4	3/8	3/8
		1400	G	G	G	1/2	0	1/4
		1500	G	G	G	1/2	0	1/4
189	180 Feldspar 120 Fe	1300	G	G	G	1/2	3/8	3/8
		1400	F	G	FG	1/2	1/2	1/4
		1500	G	G	G	0	0	1/4
190	180 Feldspar 120 Mo	1300	G	G	G	3/4	3/4	3/4
		1400	FG	G	G	1/2	1/4	3/8
		1500	G	G	G	1/2	1/2	0
191	180 Bentonite 120 Ni	1300	F	F	FF	1/2	0	0
		1400	F	F	F	0	0	0
		1500	G	G	G	1/4	1/4	1/4
192	270 Ni 30 Mn	1250	P	P	G	0	0	1/2
		1300	G	P	P	0	0	1/4
		1350	P	P	P	1/4	1/2	1/2
		1500	G	G	G	1/4	1/4	1/4
193	90 Ni 30 Mn 150 Mo	1300	G	G	G	3/4	3/4	3/4
		1400	FG	FG	G	3/4	3/4	3/4
		1500	G	G	G	3/4	5/8	1/2
198	60 Mo 225 Fe 15 Cu	1250	P	P	P	0	0	0
		1300	FF	FF	FF	1/2	0	0
		1350	FF	FF	FF	1/4	0	1/2
		1500	P	P	P	3/4	1/4	0

*P-poor, F-fair, G-good

**Torque in inch-pounds

TABLE 9

RESULTS OF COMPRESSION TESTS FROM METALLIZED DISCS
SINTERED AT 1300°C USING EXPERIMENTAL METALLIZING MIXTURES

Composition Number	Composition and Weight (gm)	Compression Load (lb) AD-94	AD-94	AL-23	Composition Number	Composition and Weight (gm)	Compression Load (lb) AD-94	AD-94	AL-23
27	210 Mo 90 Fe		1500 1100 1400 1333*		95	285 Mo 15 Lithium Titanate	900 600 1000 800*		
48	210 Mo 96.5 SiO_2 45 Mn	2300 1000 2000 1766*			124	240 Mo 24 Mn 18 Fe 9 SiO_2 9 CaO			1300 900 800 1000*
49	255 Mo 48 SiO_2 26 MnO	700 3200 1330 1733*			149	240 Mo 45 Mn 15 Fe	1700 1400 1600 1566*		
50	255 Mo 48 SiO_2 22 Mn	3000 3500 4000 3433*T	2800 3000 3800 3200*T		150	180 Mo 105 Mn 15 Fe	2200 3300 2800 2766*		
86	246 Mo 3.75 Lithium Manganate	500 550 300 450*			199	300 MoO_3	3600 1300 >5000 >2700*T	2600 2400 2400 2466*T	
89	252.5 Mo 7.5 Lithium Manganate		500 250 300 350*						

*Average

TSelected for tensile testing

TABLE 10

RESULTS OF COMPRESSION TESTS FROM METALLIZED DISCS SINTERED AT 1400°C USING EXPERIMENTAL METALLIZING MIXTURES

Composition Number	Composition and Weight (gm)	Compression Load (lb)			Composition Number	Composition and Weight (gm)	Compression Load (lb)		
		AD-94	AD-96	AL-22			AD-94	AD-96	AL-23
21	255 Mo 45 Mn	1400 1000 1400 1266*			49	255 Mo 48 SiO_2 26 MnO		3100 3600 2300 3000*T	
23	210 Mo 142 MnO_2	2800 2700 2400 2633*	1700 1000 1500 1400*		50	255 Mo 48 SiO_2 22 Mn	1900 2100 1100 1700*	2300 2300 1100 2566*T	
24	255 Mo 71 MnO_2	2800 2400 3000 2400*	1000 800 1500 1100*	1360 [illegible] 900 1570*	56	150 Mo 91 MoO_3 126 CaO	3050 2800 2200 2680*	2400 2.00 1400 1866*	
25	255 Mo 58 MnO	2400 2200 2500 2700*	1600 1200 1000 1266*		88	246 Mo 3.75 Lithium Manganate	3700 2500 3800 3333*T		
35	210 Mo 50 BaO 96.5 SiO_2			500 300 500 433*	89	292.5 Mo 7.5 Lithium Manganate	2400 1400 2500 2100*		
36	255 Mo 25 BaO 48 SiO_2	1500 1400 2000 1633*		500 1900 600 1100*	93	296 Mo 3.75 Lithium Titanate	1700 2600 2000 2100*		
38	255 Mo 31 CaO 32 Fe_2O_3	1500 1500 1500 1500*	1300 1200 1200 1233*	1600 1600 1200 1466*	94	292.5 Mo 7.5 Lithium Titanate	2300 2100 1800 2066*	1000 500 400 633*	
43	210 Mo 90 Feldspar	2600 2300 500 1800*	200 3300 1500 2300*T	1900 3500 500 1666*T	95	285 Mo 15 Lithium Titanate	2100 2300 2000 2133*		
44	255 Mo 45 Feldspar			3200 4000 2400 3200*T	96	270 Mo 30 Lithium Titanate	1900 2800 2400 2366*	800 1200 500 833*	
45	210 Mo 90 Talc			2300 2600 1600 2166*T	99	292.5 Mo 7.5 Lithium Carbonate	1500 1500 1100 1366*		
47	96.5 SiO_2 58 MnO 210 Mo		2500 2500 2500*T		100	285 Mo 15 Lithium Carbonate	800 1100 700 866*		

*Average

TSelects. for tensile testing

TABLE 10 (Cont.)

RESULTS OF COMPRESSION TESTS FROM METALLIZED DISCS SINTERED AT 1400°C USING EXPERIMENTAL METALLIZING MIXTURES

Composition Number	Composition and Weight (gm)	Compression Load (lb) AD-94	AD-96	AL-23	Composition Number	Composition and Weight (gm)	Compression Load (lb) AD-96	AD-96	AL-23
107	300 Mo	600 500 600 566*			140	240 Mo 51 Mn 9 Talc	2200 1300 2200 1900*		
128	240 Mo 51 Mn 9 Zn	2500 2000 2100 2200*			142	276 Mo 15 Fe 9 Talc	1400 2300 1000 1566*		
129	240 Mo 51 Mn 9 Ti	2600 5200 1300 3600*T			147	279 Mo 15 Fe 2 Kaolin 4 Talc	1400 1200 1000 1200*		
130	240 Mo 51 Mn 12 ZrO_2	2100 2500 2000 2200*			144	279 Mo 15 Mn 2 Bentonite 4 Kaolin	1200 1300 700 1066*		
131	240 Mo 42 Mn 9 Ti 12 ZrO_2	3400 4300 4900 4200*T	1800 2200 1600 1866*		145	240 Mo 51 Mn 6 Bentonite 3 Kaolin	2200 2200 1900 2150*		
134	240 Mo 30 Mn 30 Zn	1200 1600 1800 1533*			148	240 Mo 30 Mn 30 Fe	1300 1200 1500 1266*		
135	240 Mo 30 Mn 30 Ti	3000 4500 4200 3733*T	1800 2400 2000 2066*		153	255 Mo 60 Mn 15 $Al(OH)_3$	2500 4900 2600 3333*T		
136	240 Mo 30 Mn 41 ZrO_2	2200 3300 1906 2466*			164	240 MoO_3 60 MnO_2	3200 4800 5200 4333*T	4600 3600 4677 4100*T	
137	210 Mo 30 Mn 30 Ti 41 ZrO_2	4200 3800 3600 3866*T	2600 2500 2700 2600*T		178	150 Mo 90 MoO_3 60 MnO_2	2100 3000 4500 3333*T		
138	240 Mo 30 Mn 30 TiC	2300 1900 2900 2366*	1900 1800 2200 1900*		199	300 MoO_3	3400 2900 2500 2800*		

*Average

TSelected for tensile testing

TABLE 11

RESULTS OF COMPRESSION TESTS FROM METALLIZED DISCS SINTERED AT 1500°C USING EXPERIMENTAL METALLIZING MIXTURES

Composition Number	Composition and Weight (gm)	Compression Load (lb) AD-94	AD-96	AL-23	Composition Number	Composition and Weight (gm)	Compression Load (lb) AD-94	AD-96	AL-23
2	210 Mo 126 CaO	2400 2500 2200 2300 2350*	2100 2100 2100 2100 2100*	2100 2100 2000 2100 2075*T	25	255 Mo 58 MnO	2500 5000 2300 2500 3775*T	2700 1400 1500 1600 1800*	800 700 1600 800 975*
4	210 Mo 150 MgO	2600 2700 2700 3000 2750*			31	210 Mo 90 Ti	900 1200 1500 1000 1150*		
6	255 Mo 96.5 SiO_2			1400 2000 1800 1600 1850*	32	255 Mo 45 Ti	3600 3100 3300 3100 3350*T		
8	210 Mo 102.5 ThO_2	2300 2300 2400 2400 2350*T			39	210 Mo 45 Fe 96.5 SiO_2	1200 300 900 988*	500 800 600 633*	1600 1800 1000 1400 1450*
11	210 Mo 121 ZrO_2		2900 3000 2600 2700 2800*T		43	210 Mo 90 Feldspar K_2O Al_2O_3 SiO_2		700 1800 500 1000*	1300 1400 1500 2000 1550*
13	255 Mo 63 CaO			1750 1800 1700 1300 1785*	44	255 Mo 45 Feldspar K_2O Al_2O_3 SiO_2			1600 1000 1800 1300 1425*
22	210 Mo [illegible]	2000 2000 2100 2700 2200*			44	255 Mo 48 SiO_2 26 MnO			>5200 3500 1200 3633*T

*Average

TSelected for tensile testing

TABLE 11 (Cont.)

RESULTS OF COMPRESSION TESTS FROM METALLIZED DISCS
SINTERED AT 1500°C USING EXPERIMENTAL METALLIZING MIXTURES

Composition Number	Composition and Weight (gm)	Compression Load (lb)			Composition Number	Composition and Weight (gm)	Compression Load (lb)		
		AD-94	AD-96	AL-23			AD-94	AD-96	AL-23
50	255 Mo 48 SiO_2 22 Mn		1400 1600 1400 1466•	2200 2300 1600 2030•T	68	292.5 Mo 9.2 CeO_2	1700 2600 1900 2233•		
51	210 Mo 96.5 SiO_2 56 ZnO			2500 1000 1400 1633•	70	270 Mo 35.8 CeO_2	3000 3300 3600 3300•T		
56	150 Mo 91 MoO_3 126 CaO	2470 2300 2500 2400•	2300 2500 2500 2366•T	2800 1700 2000 2166•T	71	240 Mo 60 Ti			800 200 950•
58	150 Mo 91 MoO_3 193 SiO_2			2.30 1800 800 1600•	72	240 Mo 73.6 CeO_2	> 5000 2500 > 5000 > 4166•T	3800 3600 4000 3800•T	
62	150 Mo 91 MoO_3 121 ZrO_2	3200 2500 2500 2733•			81	292.5 Mo 8.4 BaO		1100 1000 600 720•	
65	292.5 Mo 7.5 Ti	> 5000 > 5000 > 5000 > 5000•T	2700 2900 4000 2633•T		91	270 Mo 30 Li_2MoO_3	> 5000 > 5000 1300 > 4433•T		
66	285 Mo 15 Ti	> 5000 > 5000 1200 > 6800•T	2100 2200 2100 2133•		77	240 Mo 60 Li_2TiO_3	3200 2300 3800 3133•T		
67	270 Mo 30 Ti	> 5000 > 5000 1700 > 46.•T			130	240 Mo 51 Mn 12 ZrO_2	2400 2000 2800 2400•		
					135	240 Mo 10 Mn 30 Ti	> 5200 2800 1200 > 3733•T	1600 2900 1700 1933•	
					137	210 Mo 30 Mn 30 Ti 41 MnO_2	2700 3000 2200 2633•	2200 2200 2900 2433•	

•Average

TSelected for tensile testing

TABLE 11 (Cont.)

RESULTS OF COMPRESSION TESTS FROM METALLIZED DISCS SINTERED AT 1400°C USING EXPERIMENTAL METALLIZING MIXTURES

Composition Number	Composition and Weight (gm)	Compression Load (lb)		
		AD-94	AD-96	AL-23
138	240 Mo 30 Mn 30 TiC	2700 2200 1900 2233*		
145	240 Mo 51 Mn 6 Bentonite 3 Kaolin	4100 2500 2400 3000*		
153	225 Mo 60 Mn 15 $Al(OH)_3$	3100 [illegible] [illegible] [illegible]* T		
168	240 WO_3 60 MnO_2		1400 1700 1700 1600*	
176	60 Al_2O_3 60 O'Hommel Sealing Glass #5000			1300 [illegible] 1400 1433*
176	90 Al_2O_3 90 O'Hommel Sealing Glass #5000 120 Mo	2300 2500 2500 2396*	2300 2200 2400 2300*	
134	265 Mo 15 V_2O_5	1500 1400 2200 1500*		

*Average

†Selected for tensile testing

TABLE 12

RESULTS OF COMPRESSION TESTS FROM METALLIZED DISCS SINTERED AT 1600°C USING EXPERIMENTAL METALLIZING MIXTURES

Composition Number	Composition and Weight (gm)	Compression Load (lb) AD-94	AD-96	AL-23	Composition Number	Composition and Weight (gm)	Compression Load (lb) AD-94	AD-96	AL-23
3	210 Mo 90 Mg	1200 970 1420 1167*			32	255 Mo 45 Ti	1700 2200 2300 3067*		
6	255 Mo 96.5 SiO_2	2100 1400 2000 2500*	1400 400 1400 800*	1700 1900 2100 1900*	33	210 Mo 150 TiO_2	2800 1900 1600 2100*	1000 1000 1000 1000*	
8	210 Mo 132.5 ThO_2	3100 1700 3500 2767*			34	255 Mo [illegible] TiO_2	1800 2100 [illegible] 1900*		
9	210 Mo 90 Zn	3300 [illegible] 3100 T > 3467*	1500 1000 400 967*		35	210 Mo 50 BaO 96.5 SiO_2			1400 1100 500 1000*
17	255 Mo 34 TiN_2	> 4000 2300 > 4000 - < 3100*	1400 1000 2100 1500*		43	210 Mo 90 Feldspar	2200 1200 1400 1600*	1300 1400 700 1133*	1400 1200 1800 1467*
18	255 Mo 45 Zn	3700 2300 3400 3133* T	1700 500 1000 1067*		44	255 Mo 45 Feldspar	1700 2500 2300 2100*	700 500 500 567*	1200 900 1600 1233*
19	255 Mo 56 ZnO	2100 > 4000 > 4000 T 3033*	400 1300 1700 800*		46	255 Mo 45 Talc	500 1100 900 833*	800 200 400 467*	600 900 800 767*
20	255 Mo 60 ZrO_2	> 4000 > 4000 T > 4000*	900 1000 600 833*		53	255 Mo 48 SiO_2 28 ZnO	1800 500 800 1167*	200 1000 1000 733*	900 1400 1400 1233*
21	255 Mo 45 Mn	2000 1800 2400 2066*			54	255 Mo 48 SiO_2 2. Zn			2000 1900 1500 1800*
24	255 Mo 71 MnO_2	> 4000 > 4000 > 4000 > 4000* T			57	150 Mo 91 MoO_3 150 MgO	600 800 400 600*		
25	255 Mo 58 MnO	2800 1700 2500 2100*			65	292.5 Mo 7.5 Ti	3100 2300 1600 2333*	1600 1800 2000 1800*	
31	210 Mo 90 Ti	2100 2100 2400 2200*	1200 2000 1650*	1400 2800 T 2100* T	66	285 Mo 15 Ti	2900 1200 2200 2033*	1300 1000 1000 1100*	

*Average
T Selected for Tensile Testing

TABLE 12 (Cont.)

RESULTS OF COMPRESSION TESTS FROM METALLIZED DISCS
SINTERED AT 1600°C USING EXPERIMENTAL METALLIZING MIXTURES

Composition Number	Composition and Weight (gm)	Compression Load (lb) AD-94	AD-96	AL-23	Composition Number	Composition and Weight (gm)	Compression Load (lb) AD-94	AD-96	AL-23
67	270 Mo 30 Ti	3000 3100 2900 T 3000*	1100 500 1400 1000*		104	285 Mo 15 Talc	1600 1000 2600 1733*	600 800 1200 867*	800 700 700 735*
68	292.5 Mo 9.2 CeO_2	>4000 900 1300 T >2067*	400 500 1000 633*		105	270 Mo 30 Feldspar	2200 3400 3200 2933*	800 300 500 533*	1200 1100 1600 1300*
69	285 Mo 18.4 CeO_2	2500 2800 2801 2700*	700 500 500 567*		106	285 Mo 15 Feldspar	3300 >4000 3900 T >3733*	600 900 400 633*	
70	270 Mo 36.8 CeO_2	2300 1300 1300 1967*	300 500 400 400*		107	300 Mo	3100 >4000 >4000 T >3700*	600 1500 1300 1133*	
72	240 Mo 73.6 CeO_2	1000 2100 1400 1500*	1400 1200 300 967*		108	300 Mo 0.9 Fe	>4000 2600 >4000 T >3533*		
74	296 Mo 8.6 Na_2CO_3	2000 2200 3000 2400*	1000 500 1300 933*		109	297 Mo 3 Fe	>4000 1500 T >1833*	900 1200 400 833*	
75	285 Mo 34.6 Na_2F_3	2300 800 2900 2333*			110	291 Mo 9 Fe	2300 2200 2300 2267*	800 1300 800 967*	
81	292.5 Mo 8.4 BaO	1300 1900 2100 1733*	400 700 500 533*		111	270 Mo 30 Fe	>4000 >4000 2600 T >3533*		
85	292.5 Mo 43 H_3BO_3		900 1000 1000 967*		112	300 Mo 0.9 Ni	3000 >4000 3000 T 3333*	900 800 500 733*	
86	296 Mo 21 H_3BO_3	2600 3000 2300 2633*			116	300 Mo 0.9 Co	3200 3900 >4000 T >3700*	1300 900 900 1033*	
103	270 Mo 30 Talc	1200 1200 1200 1200*	2400 300 300 1000*	1100 1000 1000 1033*	117	297 Mo 3 Co	>4000 >4000 2800 T >3600*	1200 600 500 767*	

*Average
T Selected for Tensile Testing

TABLE 12 (Cont.)

RESULTS OF COMPRESSION TESTS FROM METALLIZED DISCS SINTERED AT 1600°C USING EXPERIMENTAL METALLIZING MIXTURES

Composition Number	Composition and Weight (gm)	Compression Load (lb) AD-94	AD-96	AL-23	Composition Number	Composition and Weight (gm)	Compression Load (lb) AD-94	AD-96	AL-23
113	291 Mo 9 Co	2200 2400 1000 1200*			135	240 Mo 30 Mn 30 Ti	3200 3600 2600 3133*†	1000 800 1300 1033*	
120	300 Mo 0.9 d	> 4000 3900 > 4000 † > 3967*	1000 1400 1160 1167*		136	240 Mo 30 Mn 41 ZrO_2	2400 1900 1300 1867*	2800 1500 1300 1767*	
121	297 Mo 3 d	> 4000 > 4000 > 4000 † > 4000*	1600 1300 1501 1467*		137	210 Mo 30 Mn 30 Ti 41 ZrO_2	2600 2800 2600 2667*	1600 700 2100 1467*	1700 1800 2200 1667*
122	291 Mo 9 d	> 4000 > 4000 > 4000 † > 4000*	700 1300 1500 1167*		138	240 Mo 30 Mn 30 TiC	1600 1300 1600 1500*	600 1000 800 800*	
123	270 Mo 30 d	> 4000 > 4000 > 4000 † > 4000*	1100 900 700 900*		140	240 Mo 30 Mn 9 Talc	2300 2400 1800 2167*	900 1000 1100 1000*	1000 900 700 867*
128	210 Mo 51 Mn 9 Zn	2700 2000 1500 2733*			141	291 Mo 9 Talc	3700 3400 3900 3667*	1700 2000 2200 1967*	
129	240 Mo 51 Mn 9 Ti	1700 2500 2900 2367*			142	276 Mo 15 Fe 9 Talc	3600 3800 2900 3433*†	700 700 1000 800*	
130	240 Mo 51 Mn 12 ZrO_2	2300 1600 2600 2167*	1700 800 2400 1633		143	279 Mo 15 Fe 2 Kaolin 4 Talc	3600 3400 > 4000 > 3733*	900 1000 1300 1367*	
131	240 Mo 42 Mn 9 Ti 12 ZrO_2	2800 2400 1300 2167*	1400 700 1800 1300		144	279 Mo 15 Mn 2 Bentonite 4 Kaolin	3900 2800 2800 3500*†	900 1100 1300 1100*	
132	240 Mo 60 TiC	2800 3300 2600 2900*	1600 900 1000 1167*		145	240 Mo 51 Mn 6 Bentonite 3 Kaolin	1700 1500 1600 1600*	1200 1200 2000 1467*	
134	240 Mo 30 Mn 30 Zn	3600 > 4000 2800 > 3467*†	1700 1400 1600 1200*		153	225 Mo 60 Mn 15 $Al(OH)_3$	1700 3400 2400 2500*	1200 1400 1000 1200*	

*Average
† Calculated for Tensile Testing

TABLE 12 (Cont.,

RESULTS OF COMPRESSION TESTS FROM METALLIZED DISCS
SINTERED AT 1600°C USING EXPERIMENTAL METALLIZING MIXTURES

Composition Number	Composition and Weight (gm)	Compression Load (lb) AD-94	AD-96	AL-23	Composition Number	Composition and Weight (gm)	Compression Load (lb) AD-94	AD-96	AL-23
164	240 MoO_3 60 MnO_2	2000 1600 2900 2167*	1600 1800 1700 1700*		197	285 Mo 15 SiO_2	> 4000 > 4000 2700 T > 3567*	2700 2600 560 T 1933*	700 1000 1600 900*
175	255 Mo 30 Mn 15 Li_2CO_3	2400 1000 100 500*	2300 2200 2300 T 2300*		199	300 MoO_3	2600 2300 3600 2833*		900 800 800 767*
178	150 Mo 90 MoO_3 60 MnO_2	2800 3000 2200 2667*	2200 1700 900 1633*						

*Average
T Selected for Tensile Testing

TABLE 13

RESULTS OF COMPRESSION TESTS FROM METALLIZED DISCS SINTERED AT 1700°C USING EXPERIMENTAL METALLIZING MIXTURES

Composition Number	Composition and Weight (gm)	Compression Load (lb) AD-94	AD-96	AL-23	Composition Number	Composition and Weight (gm)	Compression Load (lb) AD-94	AD-96	AL-23
8	210 Mo 102.5 ThO_2	1,900 2700 1600 1667*	1300 700 900 967*		65	292.5 Mo 7.5 Ti		1200 2300 1750*	2700 2200 1100 - 2667*
9	210 Mo 90 Zn	1400 2600 1500 1833*			66	285 Mo 15 Ti	> 4000 > 4000 3400 T > 3467*	2100 1300 1700*	
10	210 Mo 112 ZnO	1900 2600 2200 2233*			67	270 Mo 30 Ti	2200 1600 2300 2033*	1000 800 500 767*	
16	255 Mo 75 MgO	800 1000 1800 1200*	500 700 500 567*		68	292.5 Mo 9.2 CeO_2		1600 1200 900 1233*	
17	255 Mo 51 ThO_2		900 800 1300 1000*		69	285 Mo 13.4 CeO_2	>4000 2300 2700 T 3000*	1100 1100 1300 1167*	
18	255 Mo 45 Zn	3600 3000 > 4000 > 3567*	800 200 100 367*		70	270 Mo 36.8 CeO_2		1500	
19	255 Mo 56 ZnO	3500 3200 > 4000 > 3567*	2000 1200 500 1233*		71	240 Mo 60 Zr	3000 2350 3100 2967*		
20	255 Mo 60 ZrO_2		500 900 1200 800*		72	240 Mo 73.6 CeO_2	2300 2200 1700 2067*		
31	210 Mo 90 Ti		1100 800 1800 1233*		73	292.5 Mo 17.3 Na_2CO_3	> 4000 > 4000 > 4000 > 4000* T		
53	255 Mo 48 SiO_2 28 ZnO	2900 3600 2400 2967*			78	276 Mo 6.7 K_2CO_3	> 4000 > 4000 > 4000 > 4000* T		
54	255 Mo 48 SiO_2 22 Zn	1600 2900 1500 2333*			79	285 Mo 26.6 K_2CO_3	3800 3200 1300 2767* T		

*Average
T Selected for Tensile Testing

TABLE 13 (Cont.)

RESULTS OF COMPRESSION TESTS FROM METALLIZED DISCS SINTERED AT 1700°C USING EXPERIMENTAL METALLIZING MIXTURES

Composition Number	Composition and Weight (gm)	Compression Load (lb) AD-94	AD-96	AL-23
86	296 Mo 21 H_3BO_3	3100 2200 2400 2767*		
107	300 Mo	>4000 3000 3800 >3600*T	1400 1700 2640 1900*T	
108	300 Mo 0.9 Fe	>4000 >4000 >4000 >4000*T	1700 2300 2500 2167*T	
109	297 Mo 3 Fe	>4000 3900 >3950*T	1800 700 1250*	
110	291 Mo 9 Fe	>4000 2600 1300 >3300*T	1300 800 1050*	
112	300 Mo 0.9 Ni	>4000 3400 3200 >3533*T	1300 1230 2230 1733*T	
116	300 Mo 0.9 Co	>4000 >4000 >4000*T	600 1500 1200 1267*	
117	297 Mo 3 Co	3100 3000 3050*T		
120	300 Mo 0.9 W			
121	297 Mo 3 W			
123	270 Mo 30 W			
132	240 Mo 60 TiC			
141	291 Mo 9 TaC			
186	90 Al_2O_3 90 Or Kanmal Sealing Glass #5000 120 Mo			
194	285 Mo 15 V_2O_5			

Composition Number	Composition and Weight (gm)	Compression Load (lb) AD-94	AD-96	AL-23
120	300 Mo 0.9 W	3000 2400 2600 2400*		
121	297 Mo 3 W	3700 3000 3100 3267*T		
123	270 Mo 30 W	2400 2700 3000 2800*T		
132	240 Mo 60 TiC	2600 3200 3300 3200*T		
141	291 Mo 9 TaC	>4000 2900 2500 >3133*T	1500 1000 1600 1367*	
186	90 Al_2O_3 90 Or Kanmal Sealing Glass #5000 120 Mo		2400 3300 3400 3367*T	2800 2500 2700 2667*T
194	285 Mo 15 V_2O_5		2800 1500 1600 1967*	1100 700 700 833*

*Average
T Selected for Tensile Testing

TABLE 14

SUMMARY OF COMPRESSION TEST RESULTS

Sintering Temperature	AD-94		AD-96		AL-23	
	Metallising System	Figure of Merit	Metallising System	Figure of Merit	Metallising System	Figure of Merit
1750°C	Mo-Zn	2/4	Mo	1/1	Mo-Al_2O_3-SiO_2	1/1
	Mo-Ti	2/4	Mo-Fe	1/3	Mo-Ti	1/1
	Mo-CeO_2	1/1	Mo-Ni	1/1		
	Mo-Na_2CO	1/1	Mo-Al_2O_3-SiO_2	1/1		
	Mo-K_2CO_3	1/2				
	Mo	1/1				
	Mo-Fe	3/3				
	Mo-Ni	1/1				
	Mo-Co	2/2				
	Mo-Cr	1/3				
	Mo-MgO-SiO_2	1/1				
1700°C	Mo-Zn	3/3	Mo-SiO_2	1/2	Mo-Ti	1/1
	Mo-ThO_2	1/2				
	Mo-ZrO_2	1/1				
	Mo-Mn	1/3				
	Mo-Ti	1/7				
	Mo	1/2				
	Mo-Fe	3/4				
	Mo-Ni	1/1				
	Mo-Cr	2/3				
	Mo-Cu	4/4				
	Mo-MgO-SiO_2	1/2				
	Mo-SiO_2	1/1				
	Mo-Mn-Zn	1/1				
	Mo-Mn-Ti	1/3				
	Mo-Fe-Al_2O_3-SiO_2	1/1				
	Mo-CaO_2	1/3				
	Mo-Fe-Al_2O_3-MgO-SiO_2	1/1				
	Mo-Mn-Al_2O_3-SiO_2	1/2				
1500°C	Mo-Mn	1/2	Mo-ZrC_2	1/1	Mo-CaO	1/2
	Mo-Ti	5/5	Mo-MoO_3-CaO	1/1	Mo-MnO-SiO_2	1/2
	Mo-CaO_2	2/2	Mo-Ti	1/1	Mo-MoO_3-CaO	1/1
	Mo-Li_2TiO_3	1/1	Mo-CaO_2	1/1		
	Mo-$MnTiO_3$	1/1				
	Mo-Mn-$Al(OH)_3$	1/1				
1400°C	Mo-Li_2-MnO_2	3/4	Mo-Al_2O_3-SiO_2	1/2	Mo-Al_2O_3-SiO_2	1/2
	Mo-Mn-Ti-ZrO_4	2/2	Mo-Mn-SiO_2	3/3	Mo-MgO-SiO_2	1/1
	Mo-Mn-$Al(OH)_3$	1/1	MoO_3-MnO_2	1/1		
	MoO_3-MnO_2	1/1				
	Mo-MoO_3-MnO_2	1/1				
1300°C	Mo-Mn-SiO_2	1/3	Mo-Mn-SiO_2	1/1		
	MnO_2	1/1	MoO_3	1/1		

TABLE 15

RESULTS OF TENSILE TESTS USING SPERRY'S DESIGN NO. 1
AND EXPERIMENTAL METALLIZING MIXTURES SINTERED AT 1300°C

Composition Number	Composition and Weight (gm)	Tensile Load (psi) AD-94	AD-96	AL-23	Composition Number	Composition and Weight (gm)	Tensile Load (psi) AD-94	AD-96	AL-23
50	255 Mo 48 SiO_2 22 Mn	16200 1,300 10700 13750*	15700 13200 10700 13250*	11800 7500 10450 9940*	109	300 MoO_3	4500 7190 6470 6053*	3580 4600 4300 4160*	

*Average

TABLE 16

RESULTS OF TENSILE TESTS USING SPERRY'S DESIGN NO. 1
AND EXPERIMENTAL METALLIZING MIXTURES SINTERED AT 1400°C

Composition Number	Composition and Weight (gm)	Tensile Load (psi) AD-94	AD-96	AL-23	Composition Number	Composition and Weight (gm)	Tensile Load (psi) AD-94	AD-96	AL-23
43	210 Mo 90 Feldspar		2290 9030 3580 4950*	6250 7400 9612 7690*	129	240 Mo 51 Mn 9 Ti	10400 9000 6360 8600*		
44	255 Mo 45 Feldspar		4860 3800 1220 3380	10600 7150 13000 10250*	139	240 Mo 360' Hermsal Sealing Glass #5000 19.2 Co 4.8 Sn	8700 11400 11400 10800*		
45	210 Mo 90 Talc		570 715 856 745*	7900 5720 2800 5470*	135	240 Mo 30 Mn 30 Ti	10000 11300 13200 11300*		
47	96.5 SiO_2 58 MnO 210 Mo		8440 6220 3860 6383*		137	210 Mo 30 Mn 30 Ti 41 ZrO_2	10200 9150 16700 12200*	13200 5140 10000 9780*	
49	255 Mo 48 SiO_2 26 MnO		10300 4500 4000 6430*	12800 5000 11700 9830*	153	225 Mo 60 Mn 15 $AL(OH)_3$	5800 5640 3920 5300*		
50	255 Mo 48 SiO_2 22 Mn		6000 8850 4500 6800*	14200 8950 11575*	164	240 MoO_3 60 MnO_2	9920 5000 3280 4830*	6420 10800 8500 4480*	3*10 1860 2835*
88	246 Mo 3.75 Lithium Manganate	15150 8440 9500 11300*			178	150 Mo 90 MoO_3 60 MnO_2	4640 5800 5800 5550*		

*Average

TABLE 17

RESULTS OF TENSILE TESTS USING SPERRY'S DESIGN NO. 1
AND EXPERIMENTAL METALLIZING MIXTURES ...INTERNED AT 1500°C

Composition Number	Composition and Weight (gm)	Tensile Load (psi)			Composition Number	Composition and Weight (gm)	Tensile Load (psi)		
		AD-94	AD-96	AL-23			AD-94	AD-96	AL-23
11	210 Mo 121 ZrO_2	3780 3930 6140 4610*			67	270 Mo 30 Ti	10850 14500 5270 11450*		
25	255 Mo 58 MnO	6500 6150 7200 6680			70	270 Mo 36.8 CeO_2	5350 3900 5280 5850*		
32	255 Mo 45 Ti	5640 9150 10580 8450*			72	255 Mo 73.6 CeO_2	4140 6365 4000 4840*	22000 16050 9430 15800*	
56	150 Mo 91 MnO_3 126 CaO	12500 8500 11150 10700*			91	270 Mo 30 Lithium Manganate	15550 15700 14500 15250*		
65	292.5 Mo 7.5 Ti	28400 19350 16400 21200*	6200 10000 8150 8180*		135	240 Mo 30 Mn 30 Ti	8200 15150 7630 10550*		
66	285 Mo 15 Ti	7900 12150 13900 11400*			153	225 Mo 60 Mn 15 $Al(OH)_3$	6400 7700 8320 7550*		
49	255 Mo 48 SiO_2 26 MnO			11300 11600 16100 13000*					
50	255 Mo 43 SiO_2 22 Mn			14000 16100 15200 15266*					

*Average

TABLE 14

RESULTS OF TENSILE TESTS USING SPECIFIC DESIGN NO. 1
AND EXPERIMENTAL METALLIZING MIXTURES SINTERED AT 1600°C

Composition Number	Composition and Weight (gm)	Tensile Load (lb) AD-94	AD-96	AL-23	Composition Number	Composition and Weight (gm)	Tensile Stress (psi) AD-94	AD-96	AL-23
9	210 Mo 90 Zn	11500 9730 [illegible] 8816*			109	297 Mo 3 Fe	14700 15000 [illegible] 13200*		
12	255 Mo 45 BaO	14800 11950 17200 [illegible] 14616*			111	297 Mo 3 Fe	13500 2850 [illegible] 8293*		
[illegible]	255 Mo 45 ThO_2	13500 [illegible] [illegible] 12633*			[illegible]	300 Mo 0.9 Ni	21800		
					116	300 Mo 0.9 Co	11300 [illegible] 13000*		
18	255 Mo 45 Zn	[illegible] [illegible] [illegible] [illegible]*			117	297 Mo 3 Co	2150 2870 2870 [illegible] 2330*		
19	255 Mo 45 ZnO	[illegible] [illegible] [illegible] 12700*			121	297 Mo 3 Al	18500 [illegible] 12650*		
20	255 Mo 45 TiO_2	11700 [illegible] 12550*			122	291 Mo 9 Al	3910 [illegible] 8810*		
24	255 Mo 71 MnO_2	13900 8950 [illegible] 12183*			123	270 Mo 30 Al	15900 [illegible] 10900*		
31	210 Mo 90 Ti			100 102	141	291 Mo 9 Talc	17800 16100 [illegible] 15433*		
68	272.5 Mo 9.2 $CaCO_3$	[illegible] 14300 [illegible] 11317*			143	279 Mo 15 Fe 6 Kaolin 6 Talc	16500 [illegible] 13850*		
70	270 Mo 36.8 $CaCO_3$	9050 [illegible] 7527*			144	279 Mo 15 Mo 2 Bentonite 4 Kaolin	5600 11800 [illegible] 9800*		
106	285 Mo 15 Feldspar	11950 17300 [illegible] 14616*			175	255 Mo 30 Mn 15 Li_2CO_3		12300 13400 12900*	
107	300 Mo	9450 9150 11950 10185*			197	285 Mo 15 SiO_2	4800 7180 [illegible] 9280*	2940	
108	300 Mo 0.9 Fe	14300 9300 [illegible] 11184*							

*Average

TABLE 19

RESULTS OF TENSILE TESTS USING SPERRY'S DESIGN NO. 1 AND EXPERIMENTAL METALLIZING MIXTURES SINTERED AT 1700°C

Composition Number	Composition wt. Weight (gm)	Tensile Load (psi) AD-94	AL-96	AL-23	Composition Number	Composition wt. Weight (gm)	Tensile Load (psi) AD-94	AD-96	AL-23
17	255 Mo 51 TiO_2	[illegible] [illegible] 12150*			1 7	300 Mo	1,2[illegible] 5000 [illegible] [illegible]	8[illegible] [illegible] 5150*	
18	255 Mo 45 Zn	11950 5450 [illegible] 13567*			1.9	297 Mo 3 Fe	9[illegible] 3[illegible]		
					11.	291 M. 9 Fe	163[illegible] 17[illegible] [illegible] 12150*		
19	255 [illegible] 56 [illegible]	11700 12100 13300 11600*			112	3[illegible] Mo [illegible].9 [illegible]	7.2[illegible] [illegible] 10260*	5175	
31	213 Mo 90 Ti	5[illegible] 83[illegible] 6260*			116	3[illegible] Mo [illegible].9 Co	[illegible].0 9300 1.050*		
65	292.5 Mo 7.5 Ti	1700[illegible] 1.1[illegible] [illegible] 12733*			111	277 Mo 3 [illegible]	[illegible]2600		
					186	90 Al_2O_3 90 0° Hazzel Sealing Glas. #5000 130 Mo	15600 [illegible] 12050*	6800 7600 7200*	2860
66	285 Mo 15 Ti	15700 5350 [illegible] 8400*			121	291 Mo 9 Talc	9300 11700 10500*		
[illegible]	292.5 Mo 9.2 Co [illegible]	4720 16500 12610*			117	291 Mo 3 Co	1430 2570 1985*		
70	270 Mo 36.8 CeO_2	9550							
73	292.5 Mo 17.3 Na_2CO_3	5150							
78	296 Mo 6.7 K_2CO_3	12700 1[illegible] [illegible] 8280*							

*Average

TABLE 20

SUMMARY OF TENSILE TEST RESULTS

Sintering Temperature	AD-94		AD-96		Al-23	
	Metallising System	Figure of Merit	Metallising System	Figure of Merit	Metallising System	Figure of Merit
1700°C	Mo-Th	1/1				
	Mo-Zn	2/2				
	Mo-Ti	1/2				
	Mo-CeO_2	1/1				
	Mo-Ni	1/1				
	Mo-Co	1/2				
	Mo-W	1/1				
	Mo-Al_2O_3-SiO_2	1/1				
	Mo-MgO-SiO_2	1/1				
	Mo-Fe	1/3				
1600°C	Mo-Al_2O_3-SiO_2	1/1	Mo-Mn-$LiCO_3$	1/1		
	Mo-Mn	1/1				
	Mo-W	2/4				
	Mo-Zn	2/3				
	Mo-Zr	1/1				
	Mo-Fe	2/3				
	Mo	1/1				
	Mo-Th	1/1				
	Mo-CeO_2	1/1				
	Mo-Fe-Al_2O_3-SiO_2-MgO_2	1/1				
	Mo-Co	1/2				
	Mo-SiO_2-MgO	1/1				
1500°C	Mo-MoO_3-CaO	1/1	Mo-CeO_2	1/1	Mo-Mn-SiO_2	2/2
	Mo-Ti	3/5				
	Mo-Li_2MnO_3	1/1				
	Mo-Mn-$Al(OH)_3$	1/1				
1400°C	Mo-Li_2MnO_3	1/1			Mo-Al_2O_3-SiO_2	1/1
	Mo-Co-Mn-SiO_2	1/1			Mo-Mn-SiO_2	2/2
	Mo-Mn-Ti	1/2				
	Mo-Mn-Ti-Zr	1/2				
1300°C	Mo-Mn-SiO_2	1/1	Mo-Mn-SiO_2	1/1	Mo-Mn-SiO_2	1/1

TABLE 21

RECOMMENDED METALLIZING MIXTURES

Composition Number	Composition and Weight (gm)	Sintering Temperature (°C)	Body	Peel Test Values (in.-lb)	Compression Test Values (lb)	Tensile Test Values (psi)
65	292.5 Mo 7.5 Ti	1500		2.5	>4000 >4000 >4000	20400 19350 16400
91	270 Mo 30 Li_2MnO_3	1500	AD-94	2	>4000 >4000 3300	15500 15700 14500
141	291 Mo 9 Talc ($MgO \cdot SiO_2$)	1600		4	3700 3460 3900	12300 17900 16100
72	240 Mo 73.6 CeO_2	1500	AD-96	2	3800 2500 4000	9430 22000 16050
50	255 Mo 48 SiO_2 22 Mn	1300		2	2800 3700 3800	15700 13200 10700
50	255 Mo 48 SiO_2 22 Mn	1500	AL-23	2	2200 2300 1600	14000 16100 15200
49	255 Mo 48 SiO_2 26 MnO	1500		2.75	>4000 3900 1200	11300 11600 16100

TABLE 22

ANALYSIS OF COMPARISON TEST DATA

a. All Test Data

Test Data*	Comparison Tests			
	Tensile	Compression	Drum Peel	Torque Peel
$\bar{x}$	2011.5 lb, 11061 psi	2428.0	8.08	2.844
s	559.1 lb, 3074 psi	255.8	4.97	1.353
CV%	27.8	10.5	61.4	47.57
N	61	25	103	122

b. Selected Test Data, N = 25

Test Data*	Comparison Tests			
	Tensile	Compression	Drum Peel	Torque Peel
$\bar{x}$	2080.0	2428.0	8.78	3.240
s	608.9	255.8	5.13	1.224
CV%	29.3	10.5	58.4	37.76

*Average ($\bar{x}$), standard deviation (s), coefficient of variation (CV%), and number of trials (N) for tensile, compression, drum peel, and torque peel tests. A standard 80-percent Mo and 20-percent Mn metallizing mixture, and standardized sintering and brazing conditions were used.

TABLE 23

STRESS VALUES

Seal Type	Sample Number	S_{l_o} (measured, psi)	S_{t_o} (measured, psi)	K (calculated, psi)	S_{t_o} (calculated, psi)
Ceramic-to-Nickel	N-6	-4500	6750	7400	6600
	N-9	-4800	6780		
	N-10	-1300	10550		
	N-11	- 300	11200		
	Average	-2700	8800		
Ceramic-to-Stainless Steel	S-4	-11400	19900	24300	21000
	S-5	-16500	25700		
	S-6	-11600	21700		
	S-11	-14300	20600		
	Average	-13450	22000		

*Minus sign designates compressive stress.

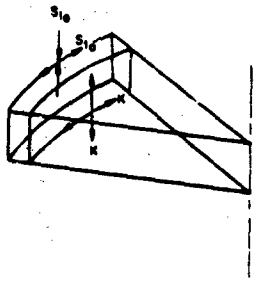

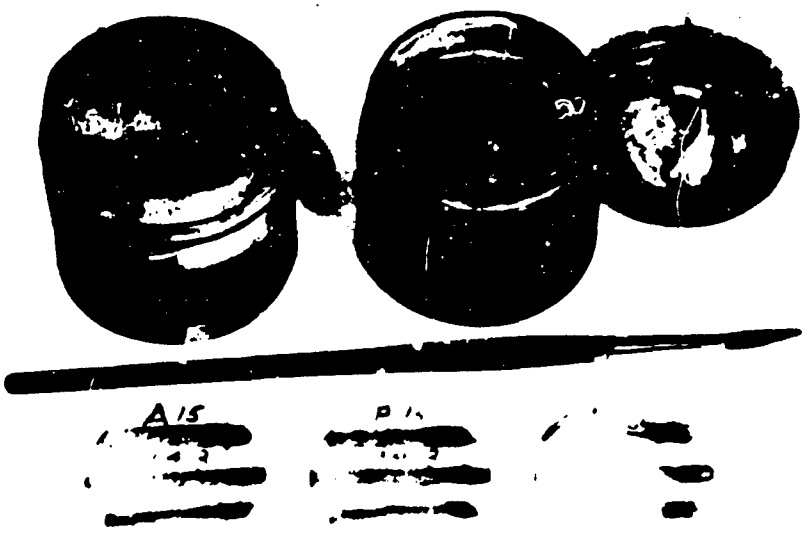

DISC A
AD-96 (COORS PORCELAIN CO)

DISC B
AD-96 (COORS PORCELAIN CO)

DISC C
DEGUSSIT AL-23
(MATERIALS FOR ELECTRONICS, INC)

FIGURE 1

METALLIZING COMPOSITIONS AS APPLIED TO TEST DISCS

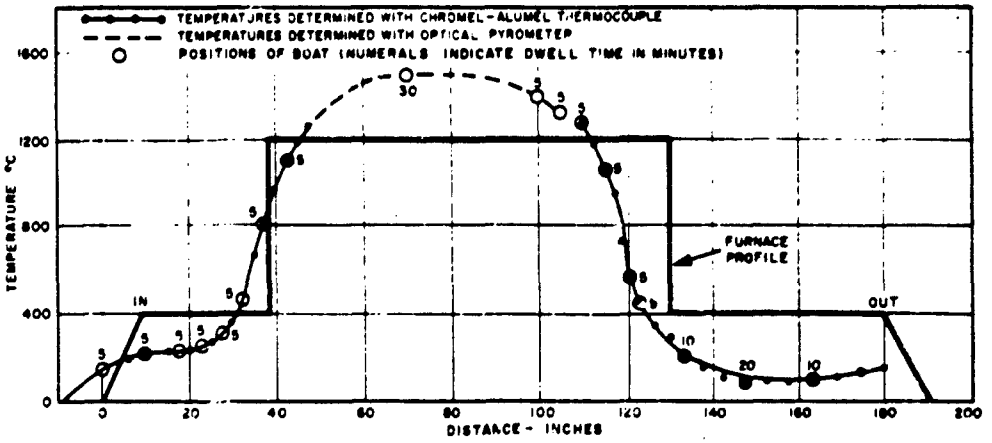

FIGURE 2

FURNACE TEMPERATURE PROFILE

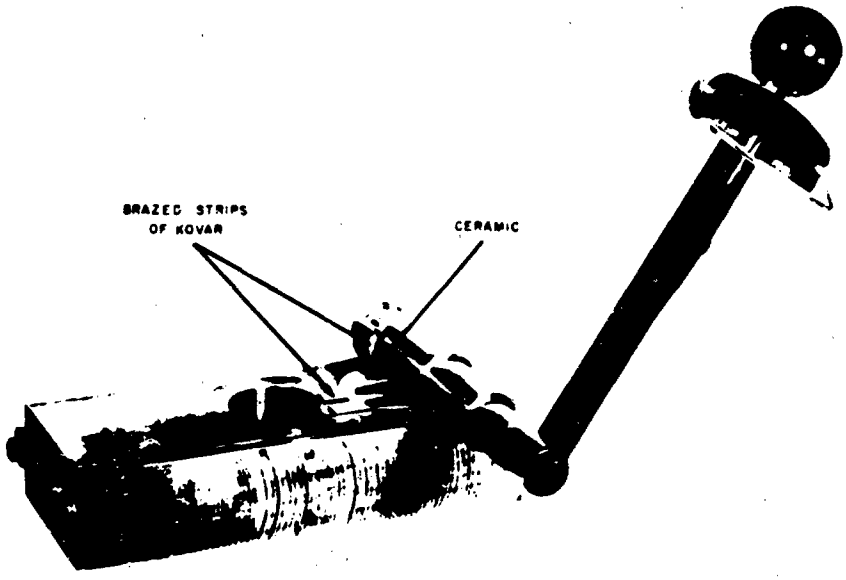

FIGURE 3
TORQUE PEEL TESTING FIXTURE

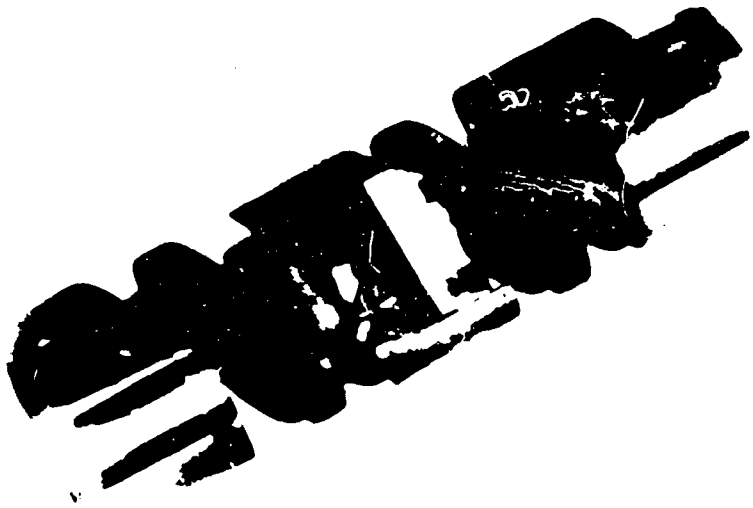

FIGURE 4

COMPRESSION TEST SPECIMEN

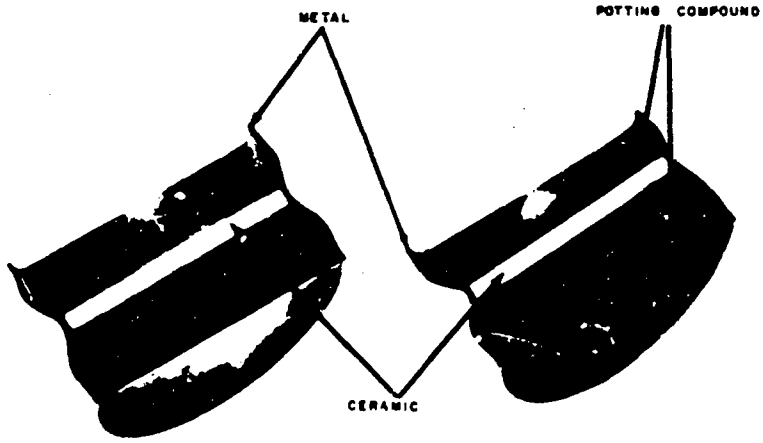

FIGURE 5

SECTIONS OF TWO COMPRESSION SPECIMENS STILL VACUUM-TIGHT AFTER DISTORTING FROM OVER 5000-POUND LOAD

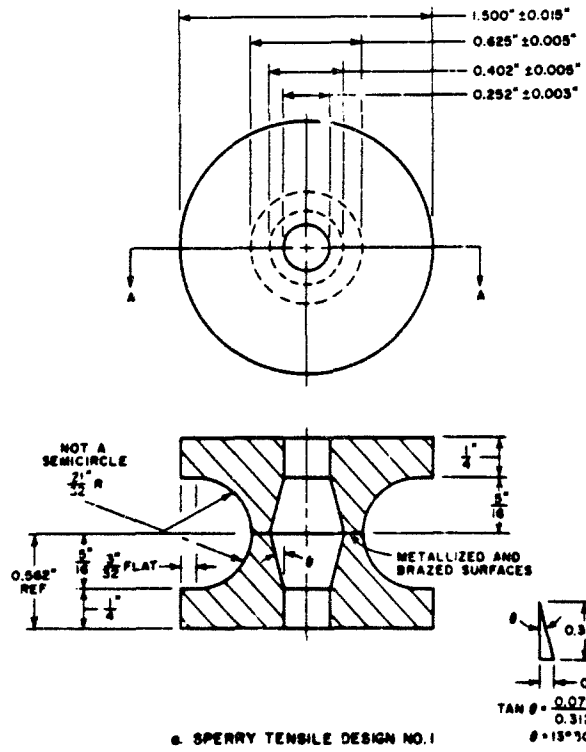

a. SPERRY TENSILE DESIGN NO. 1

b. ASTM

1

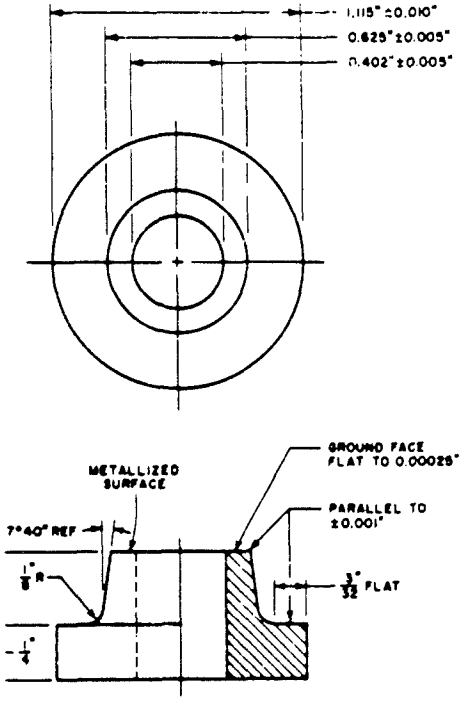

STM TENSILE TEST SPECIMEN

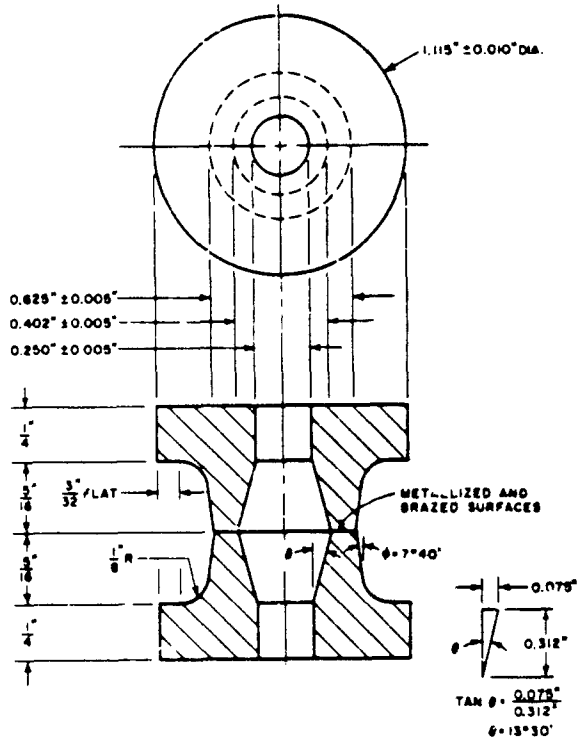

c. ASTM MODIFIED TENSILE SPECIMEN

FIGURE 6
TENSILE TEST SPECIMENS

a COORS AD-94 WITH
COMPOSITION 65 AT 1500°C
TENSILE VALUE = 28,400 PSI

b COORS AD-94 WITH
COMPOSITION 72 AT 1500°C
TENSILE VALUE = 22,000 PSI

c DEGUSSIT AL-23 WITH
COMPOSITION 50 AT 1500°C
TENSILE VALUE = 16,100 PSI

FIGURE 7

TENSILE SPECIMENS AFTER TESTING

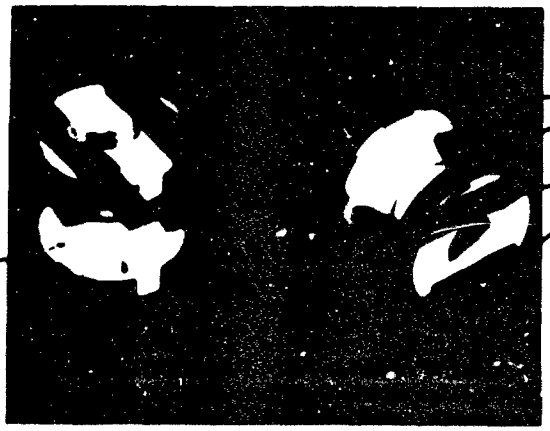

FIGURE 8

COMPARISON TEST SPECIMENS

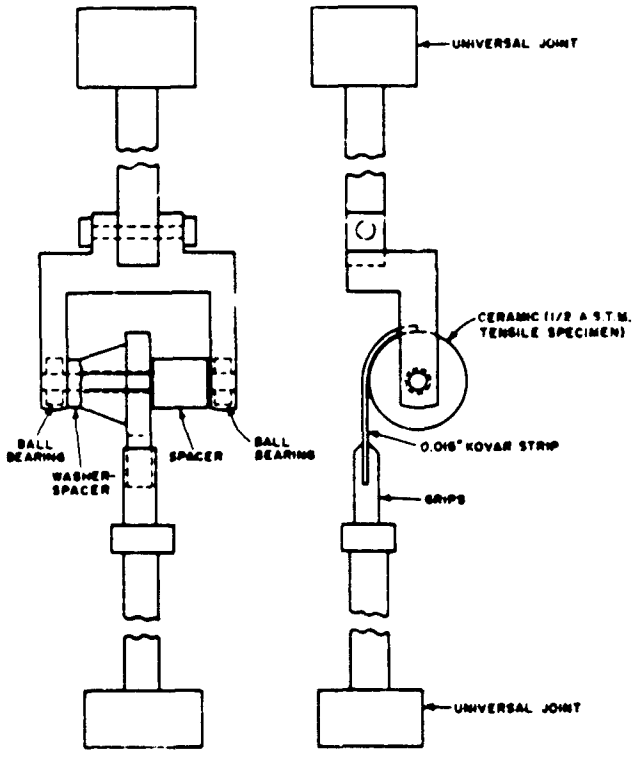

FIGURE 9

SCHEMATIC DIAGRAM OF DRUM PEEL APPARATUS

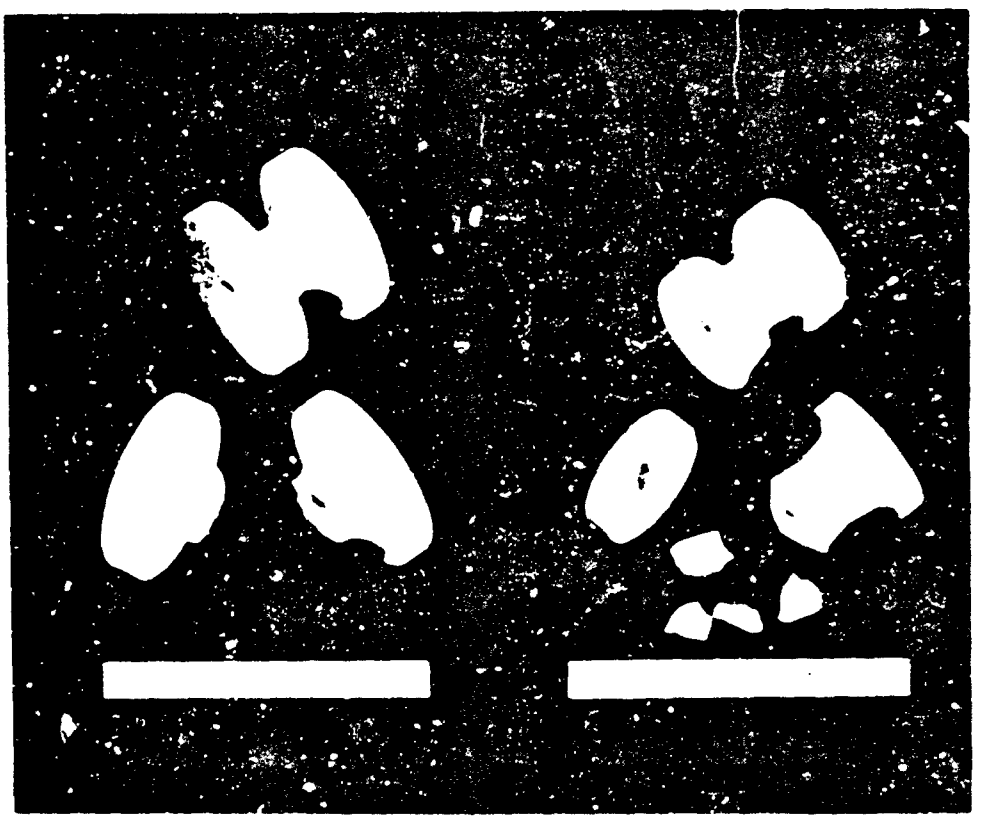

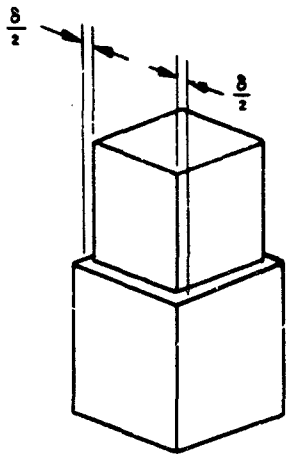

a. SEAL ELEMENT PRIOR TO BRAZING

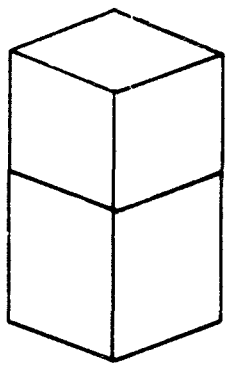

b. SEAL ELEMENT AT BRAZING TEMPERATURE

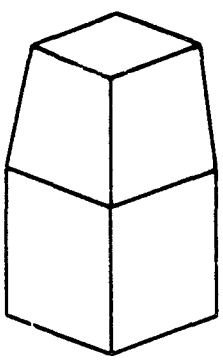

c. SEAL ELEMENT AT ROOM TEMPERATURE

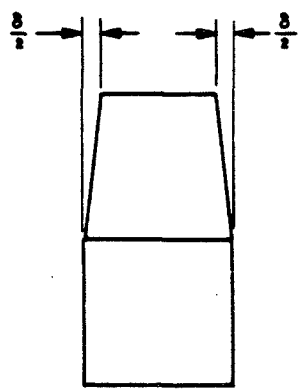

d. PLANE VIEW OF SEAL ELEMENT

FIGURE 12
SEAL ELEMENTS UNDERGOING STRESS

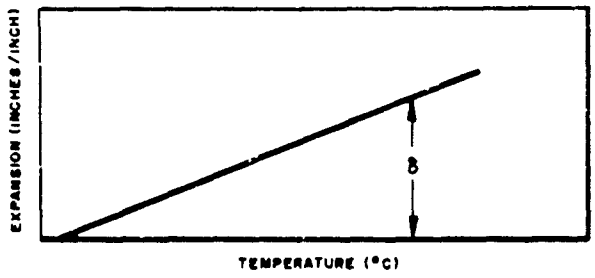

a.

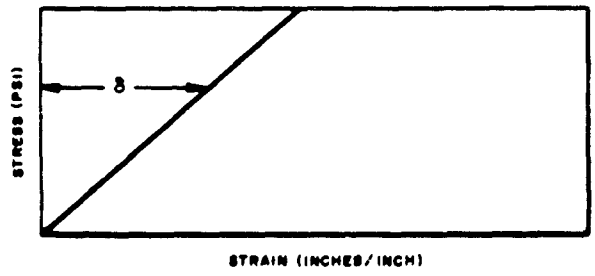

b.

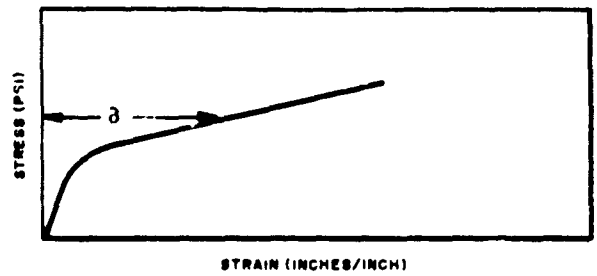

c.

FIGURE 13

STRESS-STRAIN GRAPHS

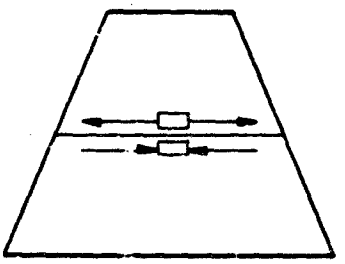

a.

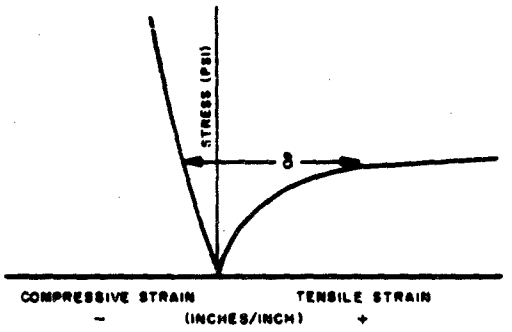

b.

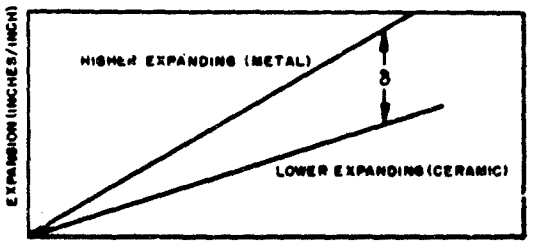

c.

FIGURE 14

STRESS-STRAIN GRAPHS

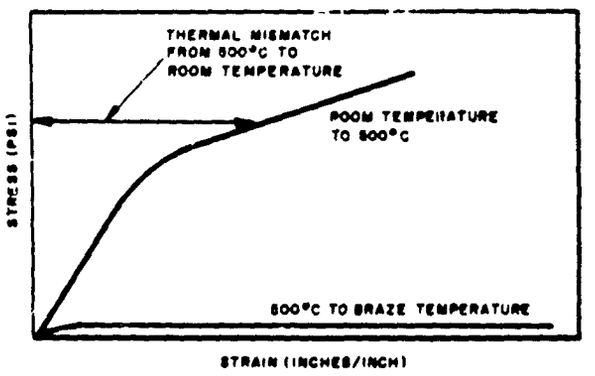

a.

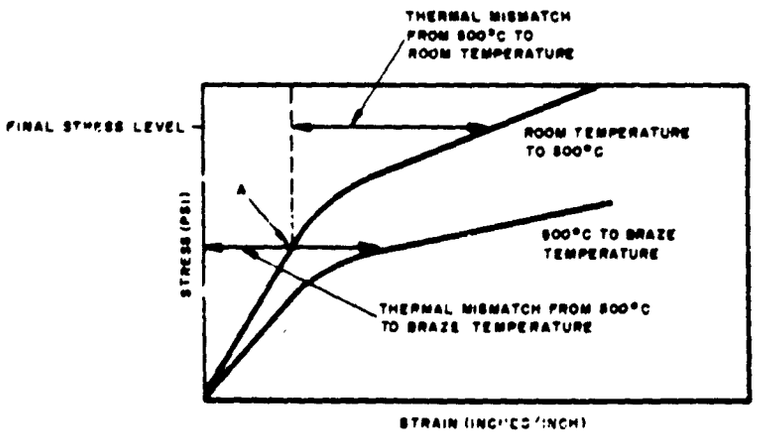

b.

FIGURE 15

STRESS-STRAIN GRAPHS

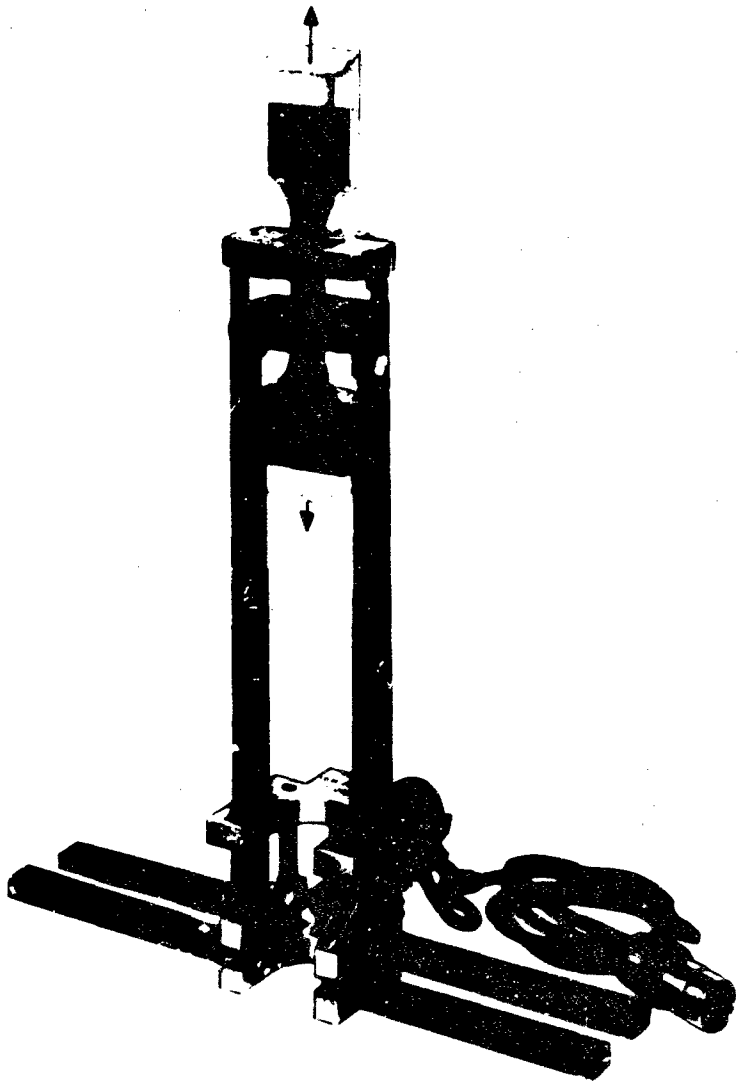

FIGURE 18

TRANSVERSE TENSILE STRESS-STRAIN SPECIMEN IN MODIFIED HIGH-TEMPERATURE EXTENSOMETER

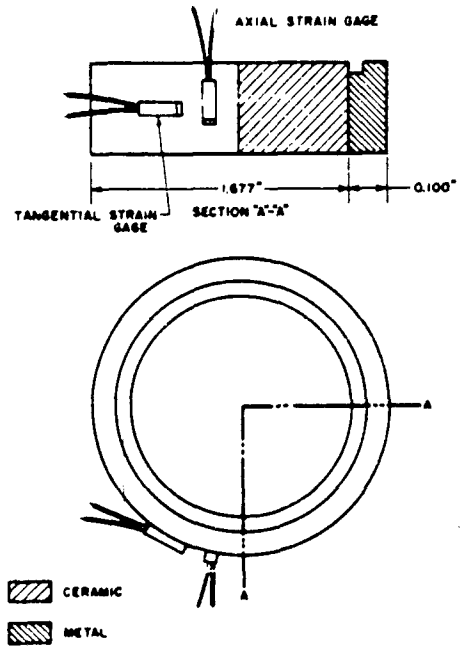

FIGURE 17

CERAMIC-TO-METAL SEAL TEST SPECIMEN FOR STRESS INVESTIGATION

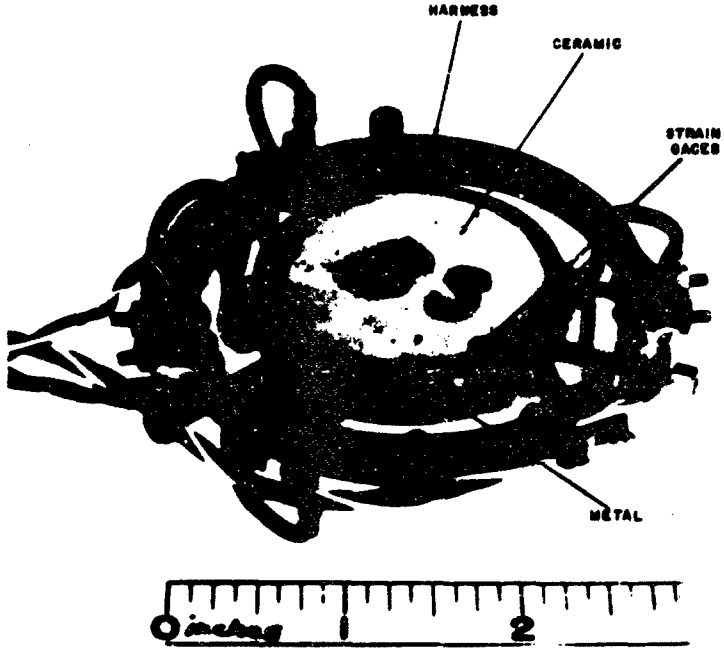

FIGURE 18
INSTRUMENTED STRESS SPECIMEN

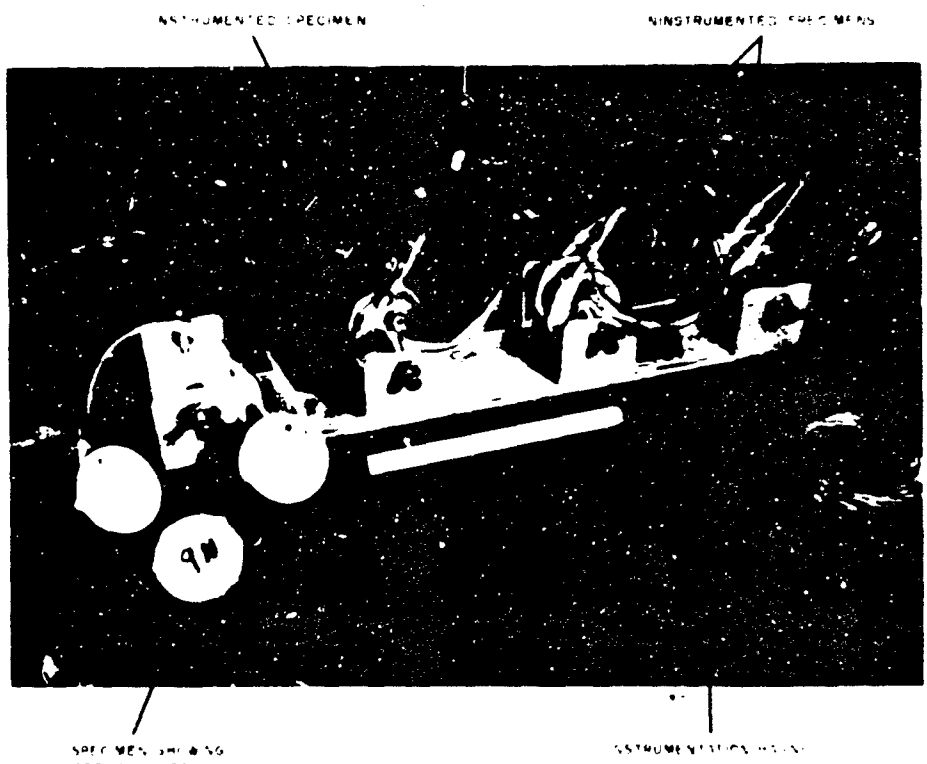

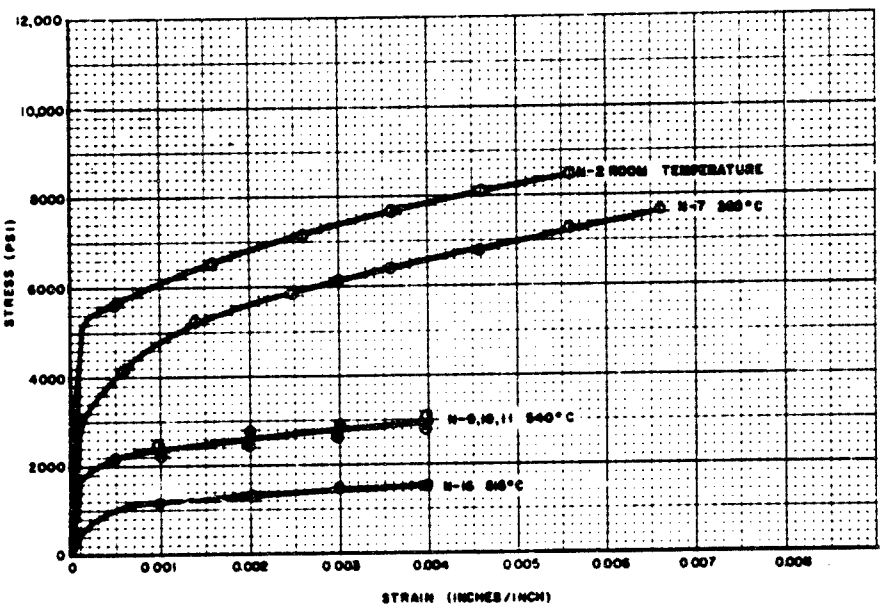

FIGURE 20

STRESS VERSUS STRAIN FOR "A" NICKEL

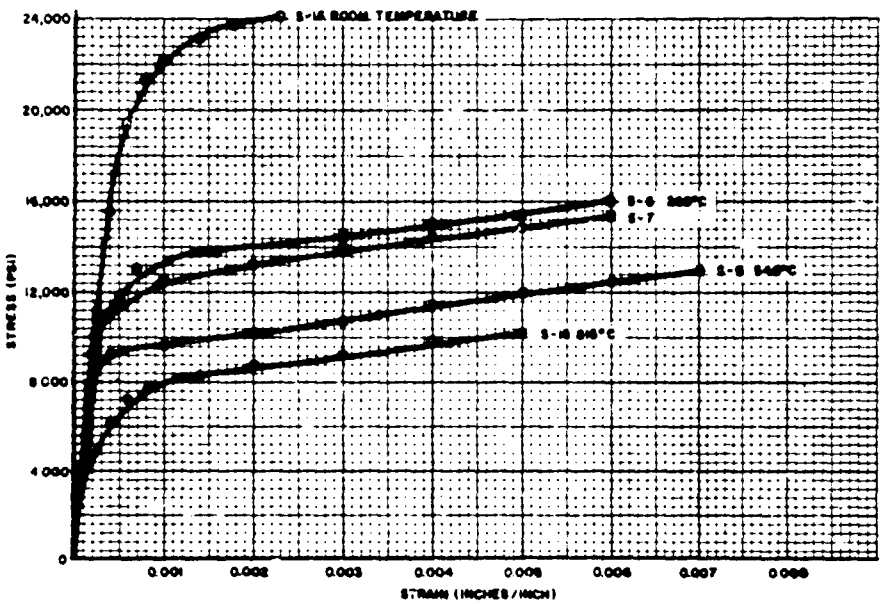

FIGURE 21

STRESS VERSUS STRAIN FOR 308 STAINLESS STEEL

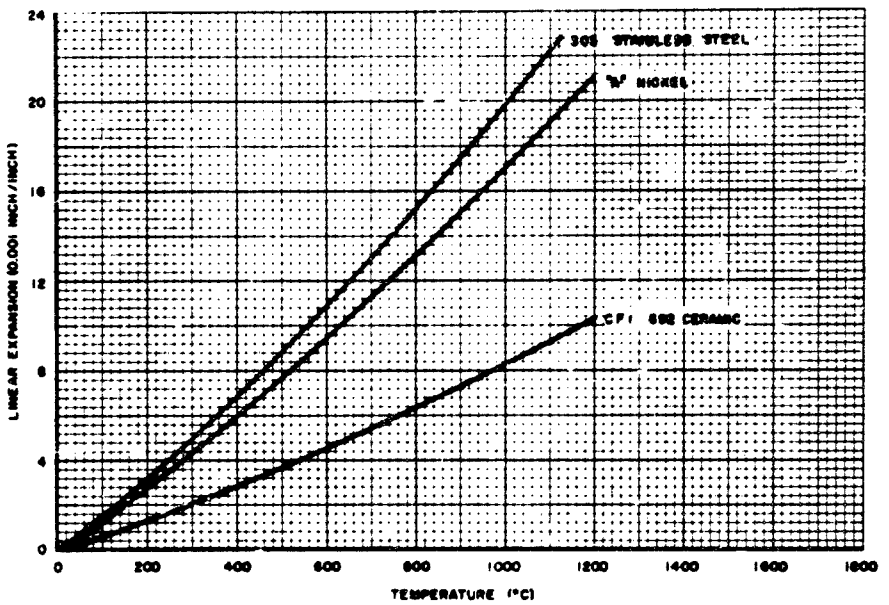

FIGURE 22

LINEAR EXPANSION VERSUS TEMPERATURE

DISTRIBUTION LIST

No. of Copies	
2	RADC (RCLTP) Griffiss AFB, New York
1	RADC (RCAT) Griffiss AFB, New York
1	RADC (RCOIL-2) Griffiss AFB, New York
10	Armed Services Technical Information Agency Arlington Hall Station Arlington 12, Virginia
1	AFCCDD (CRQSL-1) L. G. Hanscom Field, Massachusetts
2	AUL (AUL-7736) Maxwell AFB, Alabama
1	WADD (WCOSI-3) Wright-Patterson AFB, Ohio
1	Chief Naval Research Laboratory ATTN: Code 2021 Washington 25, D.C.
1	Air Force Field Representative Naval Research Laboratory ATTN: Code 1010 Washington 25, D.C.
1	Commanding Officer Signal Corps Engineering Laboratories ATTN: Technical Reports Library Fort Monmouth, New Jersey
1	RADC (RCOL, Capt. Norton) Griffiss AFB, New York
1	RADC (RCOIA, Mr. Malloy) Griffiss AFB, New York
1	Physical Electronics Labs 2493 Pulgas Avenue E. Palo Alto, California
1	Western Cold & Platinum Co. 525 Harbor Boulevard Belmont, California

DISTRIBUTION LIST (Cont)

No. of Copies	
1	Raytheon Company Waltham, Massachusetts ATTN: F. J. Fallom - Dept. 34-99
1	CO, USAS R&D Labs Fort Monmouth, New Jersey ATTN: SIGRA/SL-PRT
1	ARDC, European Office Shell Building, 60 Rue Cantersteen Brussels, Belgium
1	Secretariat Advisory Group on Electron Tubes 346 Broadway New York 13, New York
1	Polytechnic Institute of Brooklyn Microwave Research Institute 55 Johnson Street Brooklyn 1, New York
1	California Institute of Technology Department of Electrical Engineering Pasadena, California ATTN: Prof. L. M. Field
1	Harvard University Technical Reports Collection Room 303A, Pierce Hall Cambridge 38, Massachusetts ATTN: Librarian
1	University of Illinois Electrical Engineering Department Urbana, Illinois ATTN: Electron Tube Section
1	Massachusetts Institute of Technology Research Laboratory of Electronics Cambridge 39, Massachusetts ATTN: Documents Library
1	University of Michigan Engineering Research Institute 351 E. Engineering Building Ann Arbor, Michigan ATTN: J. E. Howe, Research Associates

DISTRIBUTION LIST (Cont)

No. of Copies	
1	Stanford Research Institute Menlo Park, California ATTN: Documents Center
1	University of California Electrical Engineering Department Berkeley, California ATTN: Prof. J. Whinnery
1	University of Colorado Department of Electrical Engineering Boulder, Colorado ATTN: Prof. W. Worcester
1	Johns Hopkins University Radiation Laboratory 1315 St. Paul Street Baltimore 2, Maryland ATTN: Librarian
1	Linfield Research Institute McMinnville, Oregon ATTN: Dr. W. P. Dyke, Director
1	University of Washington Department of Electrical Engineering Seattle 5, Washington ATTN: A. E. Harrison
1	Cornell University Department of Electrical Engineering Ithaca, New York ATTN: C. Dalman
1	Bell Telephone Laboratories Murray Hill Laboratories Murray Hill, New Jersey ATTN: Electronics Research Department
1	Columbia University Columbia Radiation Laboratory 538 W. 120th Street New York 27, New York
1	Eitel-McCullough, Inc. San Bruno, California ATTN: D. Priest

DISTRIBUTION LIST (Cont)

No. of Copies	
1	Federal Telecommunications Laboratories 500 Washington Avenue Nutley, New Jersey ATTN: Librarian
1	Frenchtown Porcelain Company Frenchtown, New Jersey ATTN: F. J. Hymes
1	General Electric Company Electron Tube Division of Research Laboratory The Knolls Schenectady, New York ATTN: E. L. McArthur
1	General Electric Microwave Laboratory 601 California Avenue Palo Alto, California ATTN: Dr. L. Coughanour
1	Hughes Aircraft Company Research & Development Library Culver City. California ATTN: Engineering Librarian
1	Huggins Laboratories 711 Hamilton Avenue Menlo Park, California ATTN: D. A. Roberts
1	Litton Industries 960 Industrial Road San Carlos, California ATTN: N. Moore
1	Philips Research Laboratories Irvington-on-Hudson, New York ATTN: Dr. B. Arfin
1	Polarad Electronics Corporation 43-20 34th Street Long Island City 1, New York ATTN: Vacuum Tube Engineering Department
1	Radio Corporation of America Electron Tube, Chemical & Physical Laboratory Lancaster, Pennsylvania ATTN: R. H. Zachariason

DISTRIBUTION LIST (Cont)

No. of Copies	
1	RCA Laboratories Electronics Research Laboratory Princeton, New Jersey ATTN: E. W. Herold, Director
	Raytheon Company, Spancer Laboratory Microwave & Power Tube Division Burlington, Massachusetts
1	ATTN: L. Clampitt
1	W. C. Brown
1	Sperry Rand Corporation Sperry Electron Tube Division Gainsville, Florida ATTN: P. Gergman
1	Sylvania Electronic Products, Inc. Physics Laboratory Bayside, L. I., New York ATTN: Dr. R. Hutter
1	Sylvania Electric Products, Inc. Microwave Tube Laboratory 500 E[illegible]yn Avenue Mt. V[illegible], California ATTN: Technical Library
1	Varian Associates 611 Hansen Way Palo Alto, California ATTN: Technical Library
1	Stanford University Stanford Electronics Laboratories Electron Devices Laboratory Stanford, California ATTN: D. A. Watkins
1	National Bureau of Standards Electricity and Electronics Division Washington 25, D.C. ATTN: Dr. C. P. Marsden

DISTRIBUTION LIST (Cont)

No. of Copies	
1	Ceramics for Industry Corp. Cottage Place Mineola, L. I., New York ATTN: T. S. Stanislaw
1	Coors Porcelain Company Golden, Colorado ATTN: Lawrence Farriara